

NASA CR 134786

INTERIM REPORT

DEVELOPMENT OF A 1000 V, 200 A, LOW-LOSS,  
FAST-SWITCHING, GATE-ASSISTED  
TURN-OFF THYRISTOR

BY

E. S. SCHLEGEL AND L. R. LOWRY

WESTINGHOUSE ELECTRIC CORPORATION  
RESEARCH LABORATORIES  
PITTSBURGH, PENNSYLVANIA 15235

(NASA-CR-134786) DEVELOPMENT OF A 1000V, 200A, LOW-LOSS, FAST-SWITCHING, GATE-ASSISTED TURN-OFF THYRISTOR Interim Report (Westinghouse Electric Corp.) 72 p	N75-25043
CSCL 09C G3/33	Unclas 24214

PREPARED FOR

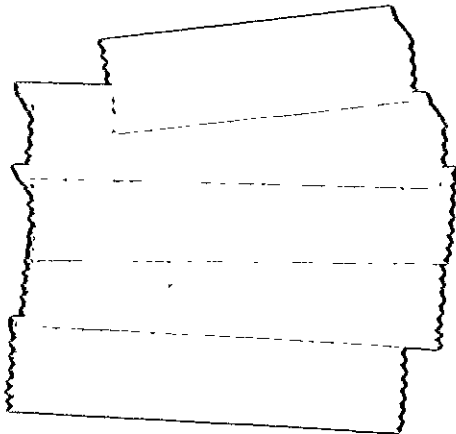
NATIONAL AERONAUTICS AND SPACE ADMINISTRATION

MARCH 31, 1975

NASA LEWIS RESEARCH CENTER  
CLEVELAND, OHIO

CONTRACT NAS3-16801  
GALE R. SUNDBERG

Reproduced by  
**NATIONAL TECHNICAL  
 INFORMATION SERVICE**  
 US Department of Commerce  
 Springfield, VA. 22151



1. Report No. CR No. 134786		2. Government Accession No.		3. Recipient's Catalog No.	
4. Title and Subtitle DEVELOPMENT OF A 1000V, 200A, LOW-LOSS, FAST-SWITCHING, GATE-ASSISTED TURN-OFF THYRISTOR				5. Report Date March 31, 1975	
				6. Performing Organization Code	
7. Author(s) E. S. Schlegel and L. R. Lowry				8. Performing Organization Report No. 75-9G5-GATT-RI	
9. Performing Organization Name and Address Westinghouse Electric Corporation Research Laboratories 1310 Beulah Road Pittsburgh, PA 15235				10. Work Unit No.	
				11. Contract or Grant No NAS3-16801	
12. Sponsoring Agency Name and Address National Aeronautics & Space Administration Washington, D. C. 20546				13. Type of Report and Period Covered Contractor Report	
				14. Sponsoring Agency Code	
15. Supplementary Notes Project Manager, Gale R. Sundberg NASA Lewis Research Center Cleveland, Ohio					
16. Abstract  Feasibility has been demonstrated for a thyristor that blocks 1000V forward and reverse, conducts 200A, and turns on in little more than 2 $\mu$ sec with only 2A of gate drive. Its features include a turn-off time of 3 $\mu$ sec achieved with 2A of gate assist current of a few microseconds duration and an energy dissipation of only 12 mJ per pulse for a 20 $\mu$ sec half sine wave, 200A pulse. Extensive theoretical and experimental study of the electrical behavior of thyristors having a fast turn-off time have significantly improved the understanding of the physics of turning a thyristor off. Thyristors of two new designs were fabricated and evaluated.  The high speed and low power have been achieved by a combination of gate amplification, cathode shunting, and gate-assisted turn-off. Two techniques for making this combination practical are described.					
17. Key Words (Suggested by Author(s)) Gate-assisted turn-off thyristor High Speed Power Thyristor Series Inverter			18. Distribution Statement Unclassified - Unlimited		
19. Security Classif. (of this report) Unclassified		20. Security Classif. (of this page) Unclassified		21. Number of Pages 72	22. Price \$3.00

**PRICES SUBJECT TO CHANGE**

\* For sale by the National Technical Information Service, Springfield, Virginia 22151

TABLE OF CONTENTS

1.	SUMMARY . . . . .	1
2.	INTRODUCTION . . . . .	2
3.	DEVICE DESIGN . . . . .	7
	3.1 Background . . . . .	7
	3.2 Design of GATT III . . . . .	8
	3.2.1 Gate Amplification . . . . .	8
	3.2.2 Cathode Edge Length . . . . .	11
	3.2.3 Shunts . . . . .	16
	3.2.4 Bypass Diode . . . . .	17
	3.2.5 Cathode Shape . . . . .	23
4.	TEST CIRCUIT DEVELOPMENT . . . . .	26
5.	PHYSICAL MODEL FOR THYRISTOR TURN-OFF . . . . .	30
	5.1 Introduction . . . . .	30
	5.2 Thyristors in General . . . . .	30
	5.2.1 A Device in Conduction . . . . .	30
	5.2.2 Current Commutation . . . . .	31
	5.2.3 Current Polarity Reversal . . . . .	31
	5.2.4 Reverse Recovery . . . . .	31
	5.2.5 Forward Voltage Reapplied (dV/dt) . . . . .	35
	5.2.6 Forward Recovery-Current-Induced IR Drop . . . . .	39
	5.2.7 IR Drop Causes Cathode Injection and Fires the Thyristor . . . . .	41
	5.3 Gate-Assisted Turn-Off . . . . .	41
	5.3.1 Carrier Sweep Out Model . . . . .	41
	5.3.2 Counteracting Voltage on p-Base . . . . .	48
	5.4 Related Considerations . . . . .	49
6.	DEVICE FABRICATION . . . . .	52
7.	EXPERIMENTAL RESULTS AND DISCUSSION OF RESULTS . . . . .	56
8.	REVIEW MEETING AND DEVICE DELIVERIES . . . . .	66
9.	SUMMARY OF RESULTS . . . . .	70

LIST OF TABLES

Table I	Target specifications . . . . .	3
Table II	Comparison of GATT I, II, and III Specifications and Achievements . . . . .	4
Table III	Process Outline . . . . .	53
Table IV	Summary of Process Runs . . . . .	54
Table V	Characteristics of the Eight Devices Loaded to NASA . . . . .	67
Table VI	Characteristics of Thyristors Delivered on NASA Contract No. NAS3-19097 . . . . .	68

## LIST OF FIGURES

Figure 1	Sketch of amplifying gate structure . . . . .	9
Figure 2(a)	Sketch of gate current path and IR drops in p-base in early stage of turn-on . . . . .	10
Figure 2(b)	Sketch of "gate amplified" current path from anode to cathode . . . . .	12
Figure 3	Switching test circuit . . . . .	13
Figure 4	Sketch of package modification with bypass diode.	19
Figure 5	Thyristor structure with an integrated bypass diode . . . . .	20
Figure 6	Top view of gate having both gate amplification and a bypass diode . . . . .	21
Figure 7	Sketch of modification of the integrated bypass diode to prevent injected electrons from firing the thyristor . . . . .	22
Figure 8	Photograph of cathode layer diffusion mask . . .	25
Figure 9	Turn-off time tester . . . . .	27
Figure 10	Model of thyristor in conduction . . . . .	32
Figure 11	Model of thyristor being commutated . . . . .	33
Figure 12	Model of thyristor with reverse current . . . . .	34
Figure 13	Model of thyristor at reverse recovery . . . . .	36
Figure 14	Model of thyristor when forward voltage is reapplied . . . . .	37
Figure 15	Model of thyristor at forward recovery . . . . .	38
Figure 16	Model of thyristor with forward-recovery-current-induced IR drops in p-base . . . . .	40

LIST OF FIGURES (continued)

Figure 17	Model of thyristor when IR drops in p-base cause cathode emission . . . . .	42
Figure 18	Model of thyristor at refiring . . . . .	43
Figure 19	The effect of the $dV/dt$ on the forward recovery current pulse height and pulse sharpness . . . . .	44
Figure 20	Earlier model for gate-assist . . . . .	46
Figure 21	Gate-assist current removes little excess charge .	47
Figure 22	Improved model for gate-assist . . . . .	48
Figure 23	Cathode patterns . . . . .	55
Figure 24	Effect of p-layer working point ( $c_w$ ) on $t_q - V_{TM}$ trade-off. . . . .	59
Figure 25	Photograph of a device made with Mask No. 3 . . .	62

## 1. SUMMARY

This interim report gives the results of a program to develop a fast high-power thyristor that can operate at ten to twenty kHz with a very low power loss. Feasibility has been demonstrated for a thyristor that blocks 1000V forward and reverse, conducts 200A, and turns on in little more than 2  $\mu$ sec with only 2A of gate drive. Its features include a turn-off time of 3  $\mu$ sec achieved with 2A of gate-assist current of a few  $\mu$ sec duration and an energy dissipation of only 12 mJ per pulse for a 20  $\mu$ sec half sine wave, 200A pulse. The significance of this type of a device is that it permits the design of a lightweight, highly efficient circuit that is suitable for both space and terrestrial applications.

The effort included an extensive theoretical and experimental study of the electrical behavior of thyristors having a fast turn-off time. Thyristors of two new designs were fabricated and evaluated. The high speed and low power have been achieved by a combination of gate amplification, cathode shunting, and gate-assisted turn-off. Two techniques for making this combination practical are described.

A comprehensive physical model for thyristor turn-off was developed that provides a basis for designing thyristors for fast turn-off both with or without gate-assist current.

The purpose and results or status of each of twelve process runs are reported. The work is continuing with emphases on three main areas -- diffusion layer profile variations, turn-on switching losses, and the development of a lighter weight package.

## 2. INTRODUCTION

The objective of this program is to design and develop a fast high-power thyristor that can operate at frequencies in the range of ten to twenty kilohertz with a very low power loss. Low power loss has always been important for aerospace applications, and it is becoming increasingly important for energy conservation in non-space applications. Operation at high frequencies is important for aerospace applications because higher frequency components are smaller in size and lighter in weight. However, it is important to consider all of the ramifications of choosing a higher operating frequency because, unfortunately, component efficiencies tend to be lower as the frequency is increased. The reduced efficiency in turn increases the weight required (1) for the larger power generation equipment to provide the extra power and (2) for the vehicle-cooling system which must dissipate the added power. Therefore, for any system, there is a frequency that will minimize the total weight. By improving the efficiency of any component at higher frequencies, the frequency-weight trade-off is improved towards higher frequency and/or lower system weight.

The target specifications for the thyristor are given in Table I. The most important feature of the new device is the ability to operate efficiently at high frequency because it dissipates less than 12 millijoules during a 20  $\mu$ sec half sine wave, 200 ampere pulse.

This contract has continued the gate-assisted turn-off thyristor (GATT) development programs of contracts NAS12-2198 and NAS3-14394. A comparison of the objectives and achievements of the three contracts is given in Table II.

The background that lead to the work on this contract was described in NASA Reports No. CR-120832 and No. CR-121161, which are the



TABLE I  
Target Specifications

Symbol	Description	Specifications
$V_{RRM}$	Minimum reverse blocking voltage.	1000V
$V_{DRM}$	Minimum forward blocking voltage.	1000V
$I_{T(rms)}$	Maximum rms forward current.	200A
$V_{TM}$	Maximum steady state forward voltage drop for conduction of 200A.	2.5V
$t_{on}$	Time required to reach $V_{TM}$ after initiation of current conduction with a rate of rise of 100A per microsecond and application of a gate signal of 2.0A for ten (10) microseconds.	2 $\mu$ sec
$I_{RRM}$	Maximum reverse leakage current at 1000V.	10 mA
$I_{DRM}$	Maximum forward leakage current at 1000V.	10 mA
$I_G$	Maximum gate current to fire at $V_{DRM} = 30V$ .	200 mA
$V_G$	Maximum gate voltage to fire at $V_{DRM} = 30V$ .	4V
$I_h$	Minimum holding current.	200 mA
$t_q$	Maximum time after anode current has reached zero before anode voltage can be reapplied @ the maximum rate of rise of voltage (dV/dt) as stipulated below and a maximum gate signal of 2.0A for 3 $\mu$ sec.	3 $\mu$ sec
dV/dt	Maximum rate of rise of anode voltage.	400V/ $\mu$ sec
E pulse	Allowed dissipation per pulse (20 $\mu$ sec half sine wave with a 200A peak).	12 mJ
dI/dt	Maximum rate of rise of current concurrent with and after a gate signal of not more than 3.0A.	100A/ $\mu$ sec

TABLE II  
Comparison of GATT I, II, and III  
Specifications and Achievements

Parameter, Units	1969-1970 GATT I Specs [Achieved]		1971-1972 GATT II Specs [Achieved]		1973-1974 GATT III Specs [Achieved]	
	Current rating, A	50	50	100	100	200
$V_{DRM}$ , V	600	600	1000	1000	1000	1000
$V_{RRM}$ , V	600	600	1000	1000	1000	1000
$V_{TM}$ , V @ a current of	2.0	2.0 50A	2.0	2.0 100A	2.5	2.5 200A
$t_{q@}$ , $\mu\text{sec}$	2.0	2.0 100°C, 50A 10A/ $\mu\text{sec}$ , 400V/ $\mu\text{sec}$ gate: -14V, 0 $\Omega$	2.0	2.0 100°C, 100A 25A/ $\mu\text{sec}$ , 400V/ $\mu\text{sec}$ gate: -20V, 1 $\Omega$	3.0	3.0 100°C, 200A 25A/ $\mu\text{sec}$ , 400V/ $\mu\text{sec}$ gate: 2A
$dV/dt$ , V/ $\mu\text{sec}$ with gate	400	400 -10V through 10 $\Omega$	400	400 -10V through 10 $\Omega$	400	400 open
$dI/dt$ , A/ $\mu\text{sec}$	10	10	400	75	100	100
$I_{GT}$ , A			0.2	0.5	0.2	0.2
$V_{GT}$ , V			4.0	1.0	4.0	1.0
$I_H$ , mA			25	200	200	200
$t_{on}$ , $\mu\text{sec}$ with gate drive of and $dI/dt$ of			2.0 2.5A 100A/ $\mu\text{sec}$	3.0 15A	2.0 2.0A 100A/ $\mu\text{sec}$	~ 2 2.0A
E pulse, (dissipation per pulse), mJ					12	12

Final Reports for the two preceding GATT development contracts. The device is to be used in a series inverter circuit for the conversion of dc power from one voltage level to another. Regulation is provided to maintain the output voltage constant independent of changes in the input voltage or output loading. The use of natural commutation minimizes the current and voltage transients thereby increasing the efficiency and reliability of the circuit; it also minimizes electromagnetic interference problems. The size, weight, and cost of a circuit can be decreased if the operating frequency can be increased. One limit on the upper frequency of circuit operation is the turn-off time of the thyristor. The turn-off time can be reduced by the application of a negative gate current while the thyristor is being turned-off. Such a GATT was the object of all three contracts.

Other work on GATT devices includes an experimental 600V, 100A GATT, with a  $t_q$  of 2  $\mu$ sec made by the Westinghouse Brake and Signal (type D1171), and a 1000V, 400A GATT with a  $t_q$  of 10  $\mu$ sec made by the Mitsubishi Electric Corporation.

The scope of the present work included:

1. A broad review of the possibilities by which the turn-off time and energy loss per pulse might be decreased.
2. An experimental study of the electrical behavior of fast turn-off thyristors.
3. The development of a better model for gate-assisted turn-off.
4. The design and fabrication of a new family of GATT devices based on the improvement in understanding of thyristor turn-off.
5. The evaluation of devices of this new design.

The information reported herein provides both a theoretical understanding, and an empirical measure, of the present state-of-the-art of high-voltage, high-current, GATT's. This information can be used by those involved in the design of low-loss, high-power, high frequency circuits of the type described by Schwarz.<sup>(1)</sup> The importance of power systems using thyristors that have higher speed, power handling capability, and efficiency increases as the price and availability of fossil fuels force more and more energy to be used in the form of electric power.

A precise definition of the purpose of this effort includes:

1. The design and development of a high-power, gate-assisted turn-off thyristor with the characteristics described in Table I.
2. The fabrication and delivery of 25 thyristors which demonstrate the achievement of (1).
3. The identification of research problem areas to be solved in order to significantly extend the performance level of GATT's.

The work was done by investigators of the Research Laboratories of the Westinghouse Electric Corporation, Pittsburgh, Pennsylvania, in cooperation with the Westinghouse Semiconductor Division, Youngwood, Pennsylvania. Thyristors were fabricated in the production facilities of the Semiconductor Division using modifications of standard production processes. Special modifications and all device testing and behavioral studies were conducted at the Research Laboratories.

The value of the work done was significantly enhanced by direct interaction, encouraged by NASA, with those at TRW who were involved in the development of a circuit in which these thyristors are to be used.

### 3. DEVICE DESIGN

#### 3.1 Background

The preceding work, performed by Westinghouse Electric Corporation and supported by NASA, <sup>(2,3)</sup> can be summarized as follows.

The first GATT development program, from the middle of 1969 to the middle of 1970, resulted in the demonstration that devices could be made that blocked 600V, carried 50A of average anode current with a  $V_{TM}$  of no more than 2V. They had a turn off time,  $t_q$ , of 2  $\mu$ sec tested with a gate-assist gate bias of -10V in series with 10 ohms, all measured at 100°C. The cathode-emitter was of mesa construction and, therefore, had widely varying leakage currents between individual emitter fingers. To produce usable devices with this process, it was necessary to test each emitter finger individually and to weld a raised contact to each individual good finger so that the device could be packaged without contacting the leaky fingers. This was clearly not a good manufacturable design.

The second GATT development program, from about September 1971 to November 1972, yielded devices that blocked 1000V and carried 100A of average anode current with a  $V_{TM}$  of no more than 2V. The turn-off time was less than 2  $\mu$ sec, tested with a gate-assist bias of -20V through a gate-assist source impedance of no more than 1 ohm. The measurements were taken at 100°C. This device was planar and manufacturable, but it had five disadvantages:

1. To achieve the desired turn-on speed, the gate turn-on current had to be > 15A.
2. To achieve the desired turn-off time, the gate assist current had to be > 10A.

3. If this high level of gate-assist current was applied before the anode current had been commutated to zero, the thyristor was likely to be permanently damaged.
4. The energy loss per pulse was quite high, e.g.,  $\sim 30$  mJ. This is a result of a desire by the circuit designer to use gate currents that are no greater than a few amperes.
5. A constant gate bias was necessary to prevent firing of the device at a low  $dV/dt$  level. Without a gate bias, the  $dV/dt$  rating was much lower than the specified  $400V/\mu\text{sec}$ .

### 3.2 Design of GATT III

#### 3.2.1 Gate Amplification

In order that the device be turned on in two microseconds with an external gate drive of only two amperes, it is absolutely necessary that gate amplification be used. Gate amplifier structures, of the form sketched in Fig. 1, are in general use throughout the industry on many types of thyristors that are not to be operated in the gate-assist mode.

The operation of the amplifying gate structure can be briefly described as follows:

When a positive current is fed into the gate, and out through cathode, it has a path shown in Fig. 2(a). This causes IR voltage drops in the p-base under both the auxiliary and the main cathodes. Because of the much shorter edge length of the auxiliary cathode, and the roughly equal cathode line widths of the two cathodes, the IR drop under the auxiliary cathode is much higher than that under the main cathode. When the IR drop under the auxiliary cathode reaches about 0.7 to 0.9V, the edge of the auxiliary cathode that faces the gate is forward biased

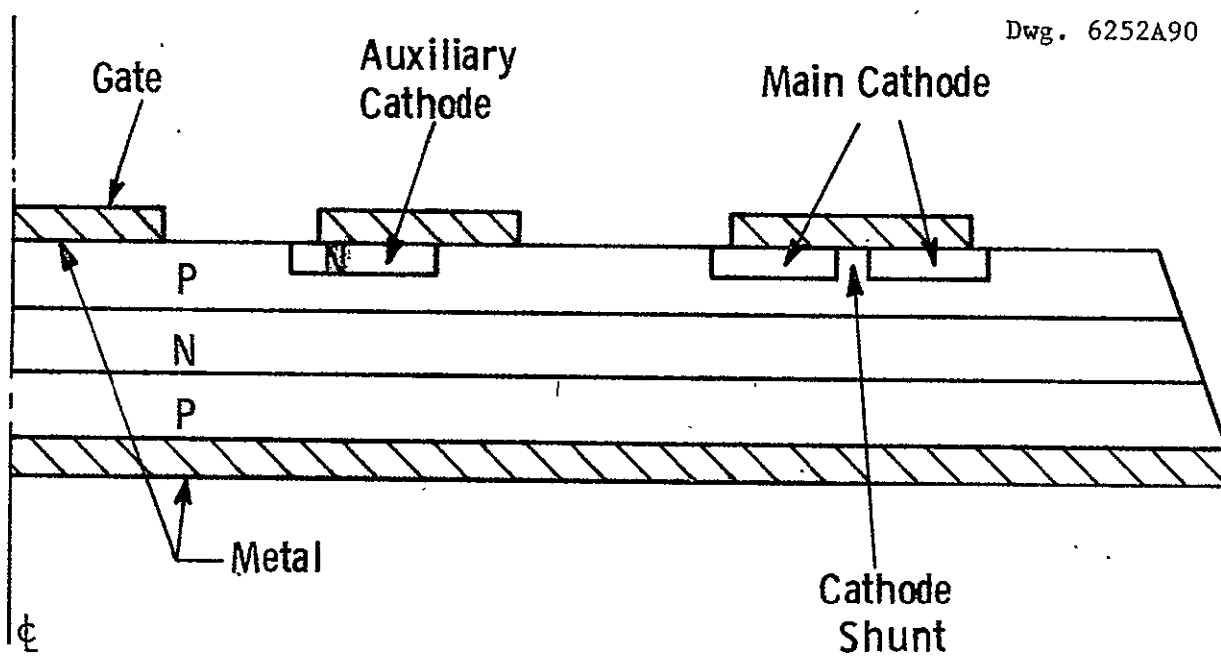


Fig. 1—Sketch of amplifying gate structure

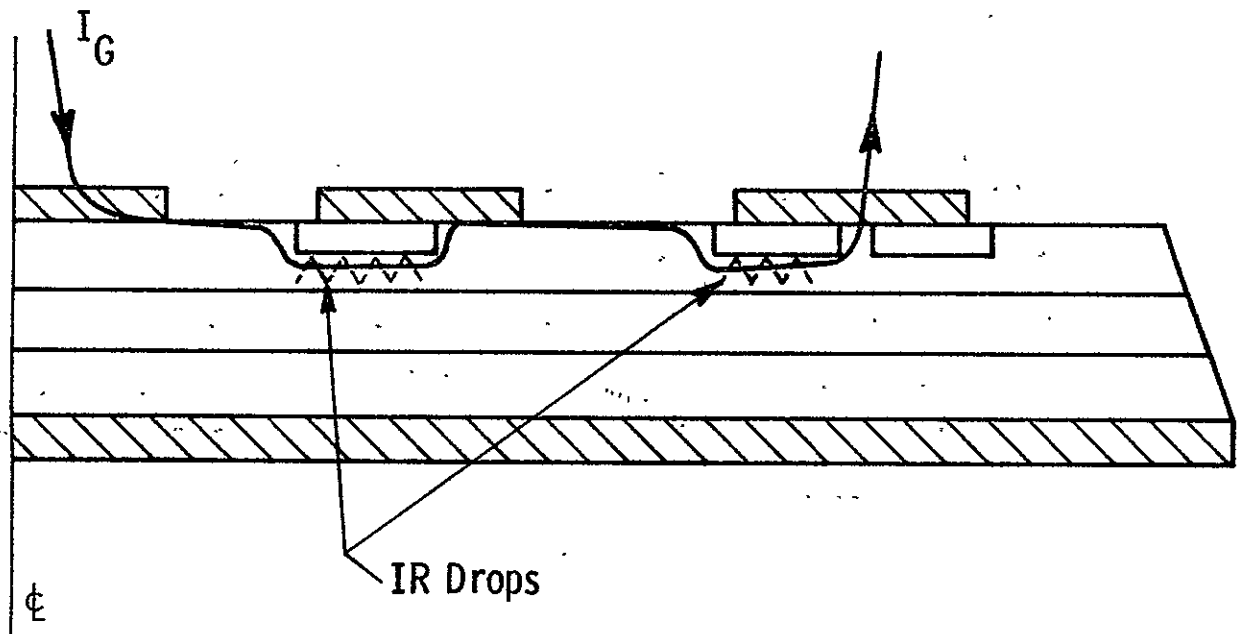


Fig. 2a—Sketch of gate current path and IR drops in P-base in early stage of turn-on



to a degree sufficient to cause thyristor action. This renders the auxiliary thyristor conductive and provides a path, as shown in Fig. 2(b), for relatively high current from the anode, through the auxiliary thyristor, through the floating gate and through the p-base under the main cathode and out through shunts of the main cathode. This high "amplified" gate current produces a high IR drop under the main cathode and in the same manner as that of the firing of the auxiliary thyristor, fires the main thyristor very rapidly. The rapidity of the firing causes the thyristor to pass through its lossy transient state quickly and, thereby, makes for a low turn-on switching loss per pulse.

### 3.2.2 Cathode Edge Length

The question that was most difficult in the design of this device was: what is the best length for the periphery of the auxiliary and of the main cathode for the lowest turn-on switching loss under the given operating conditions? More specifically, would an increase in cathode edge length,  $L_{gc}$ , for a given gate current drive:

1. Increase the energy loss because the gate drive per unit length is reduced, thereby causing a slower turn-on;
2. Decrease the energy loss because the current density and, therefore, the forward drop are lower at each current level; or
3. Cause no change in the energy loss because the effects of (1) and (2) cancel out?

The results of a considerable amount of effort in this area can be summarized as follows:

1. During the first few months of the program, anode voltage and anode current waveforms were measured on the circuit sketched in Fig. 3. This circuit switches the thyristor on from an anode voltage of 200V. The circuit limited  $dI/dt$  could be varied from 10 to 250 A/ $\mu$ sec by

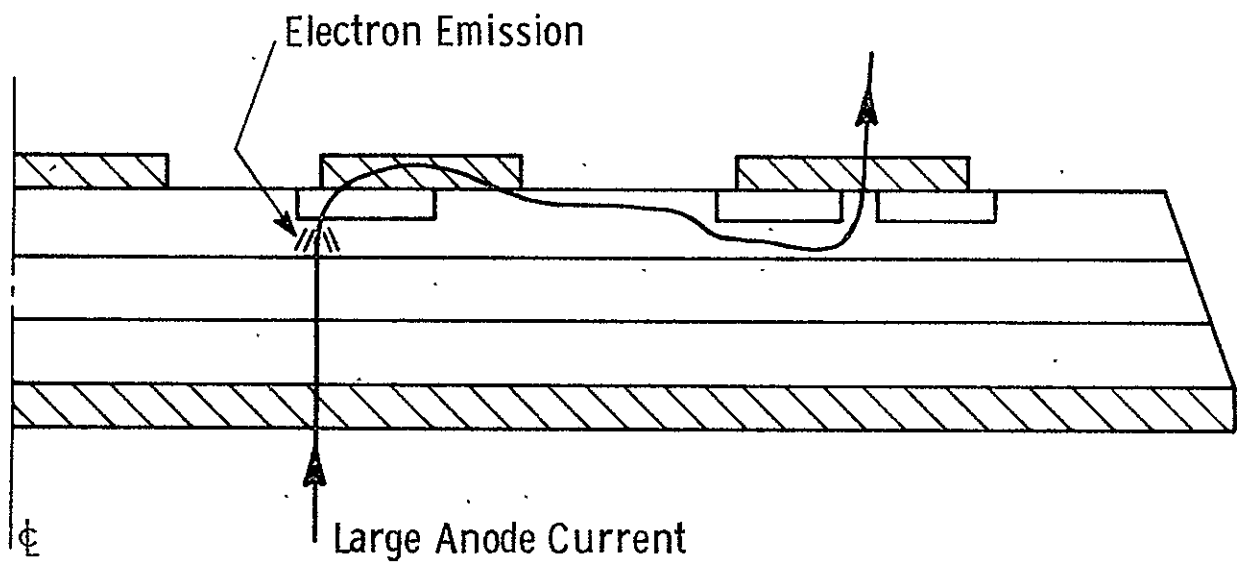


Fig. 2b—Sketch of "Gate Amplified" current path from anode to cathode

13

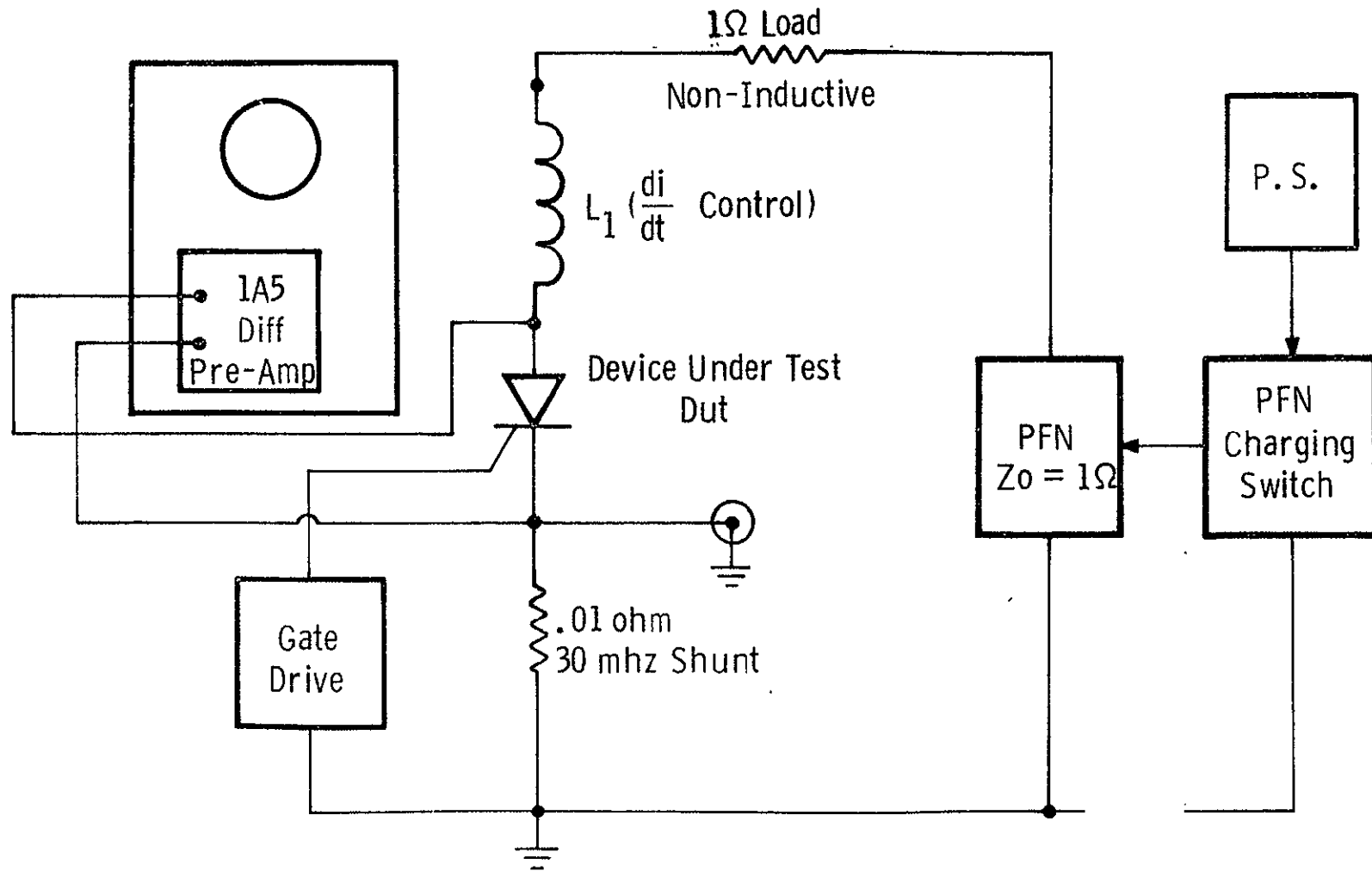


Fig. 3- Switching test circuit

changing the inductance  $L_1$ . The devices were tested at room temperature. Four devices having cathode edge lengths of 1.6, 8.2, 23, and 30 cm were measured. The gate drive current (unamplified) was varied from 6 to 24 amperes. The resulting data showed no well-defined dependence of the turn-on speed and losses on the length of the cathode boundary.

Possible reasons for the failure of this work to provide a definitive result include:

- a. There is always uncertainty in the accuracy of a small ( $\sim 3V$ ) voltage being measured within a few tenths of a microsecond after a much higher voltage ( $\sim 200V$ ) was present on, and saturating, the amplifier of the oscilloscope.
- b. It is difficult to be certain that no emf's are developed in the voltage probe leads in the vicinity of the line in which a  $dI/dt$  of the order of  $10^8 A/sec$  exists.
- c. Other variables such as the shunt patterns and the spacing between the shunt and the edge of the cathode were different. Also the diffusion profiles may have been different.
- d. The sample size was small, one device for each cathode edge length, because of the limited amount of time for such work.

2. To minimize the effects of uncontrolled variables, the following technique was developed by which the effects of varying the cathode edge length can be simulated on a single device. To understand this approach, consider the following thought experiment. Take two identical thyristors and compare how one of them would behave while being turned on in a given circuit with a given set of conditions with how both would behave, perfectly paralleled, in the same circuit with the same conditions.

The device would see the following differences:

- a. In the parallel case, both the gate-drive-current, and the anode-current, densities per unit of cathode edge length would be half their values in the single-device case.
- b. The losses in the parallel case occur over twice the cathode edge length of that of the single device case.

Note that, if the loss per unit of edge length were the same in both cases, the total loss in the second case would be twice that of the first case. Based on this, one should be able to test a single device under two proportionate sets of gate current drive and circuit-limited-anode  $dI/dt$  to simulate differences in cathode edge length. The losses measured under the two sets of currents must be scaled in proportion to the simulated difference in cathode edge length. Turn-on losses were measured using this technique, and again the results were not definitive.

Possible reasons for this lack of a definitive result are:

- a. The accuracy of the voltage measurement has not been improved.
  - b. The premise on which this technique is based is that both the gate and anode currents are circuit and not device controlled. The validity of this premise was not established.
3. Not having found a clear indication of an effect of the cathode edge length on the turn-on behavior in the efforts described above, the new thyristor was designed to have the best turn-off time. Turn-on considerations imposed no limitations in the design, and the precise effect of the new design on the turn-on behavior could not be predicted.
4. Near the end of the program, in October 1974, at the IAS Meeting of the IEEE, P. Voss gave a paper<sup>(4)</sup> that re-emphasizes

the importance and difficulties of developing a better understanding of turn-on behavior. Dr. Voss reported that there is a critical current density ( $\sim 5A/cm$  in his devices) per unit of cathode edge length at which the device turns on. (By turns on, he means that the circuit, rather than the device begins limiting the anode current and the anode current rises rapidly and the anode voltage falls rapidly.) Dr. Voss' extensive work still leaves important areas to be studied:

- a. He studied the uniformity, or lack thereof, of IR light emission during turn-on; and it is not known how this relates to transient energy losses.
- b. There is still the question of how to measure turn-on losses accurately.
- c. Can a good model for turn-on behavior be developed similar to that for turn-off behavior given in Section 5 of this report?

Clearly an intensive systematic effort is called for in these areas, based on the work already completed in this program and on Dr. Voss' work, to develop a good understanding of turn-on and its dependence on such variables as  $dI/dt$ , gate drive, cathode edge length, anode voltage switched from, temperature, etc.

Further studies in these areas are to be performed in the extension of this contract that has recently been negotiated.

### 3.2.3 Shunts

In contrast to the previous GATT designs, the new GATT designs use a shunted cathode for three reasons:

1. The gate-assist current specification calls for a gate pulse only during the turn-off period. Shunts are necessary to prevent firing of the device by  $dV/dt$  during the longer proportion of the time when there is no gate-assist current present.

2. The previous (unshunted) GATT's were subject to failure if the gate-assist current was applied before the commutated anode current reached zero. This failure mode is commonly found in gate-controlled switches and involves current crowding in the middle of unshunted cathode lines. The presence of shunts prevents this type of failure.
3. It was recognized from the beginning that it would be desirable to meet the objectives of the contract without the need for a gate-assist current. The only way this might be achieved is to have a shunted cathode—because of the need for a 400V/ $\mu$ sec  $dV/dt$  rating.

#### 3.2.4 Bypass Diode

The combination in a single thyristor of gate amplification and gate-assisted turn-off or gate turn-off (GTO or GCS) confronts one with a problem. In order for a low gate current, of say 50 mA, to turn a thyristor on, the resistance in the p-base under the auxiliary cathode must be at least  $0.7V/0.05A = 14\Omega$ . (The 0.7V is the voltage needed to cause the cathode to start emitting.) On the other hand, when the thyristor is to be turned off with a gate-assist current of 2A, as called for in the contract, this 2A through 14 ohms of resistance produces an IR drop of 28V. (The need for a much larger gate current at turn-off than at turn-on is because only the turn-on current can be amplified.) This is well over the voltage at which the cathode junction avalanches. The high energy density in this avalanche is enough to melt silicon and degrade the auxiliary cathode junction.

To overcome this problem, it is necessary to bypass the resistance of the p-base under its auxiliary cathode when gate-assist current is drawn. On this contract, this has been achieved by two different approaches.

In one approach, which was developed on a separate Westinghouse program, a small diode is soldered in the package as shown in Fig. 4. This diode contacts to the main gate and the floating gate as shown. This diode carries a negligible amount of forward current when turn-on current is applied to the main gate. On the other hand, when gate-assist current is drawn from the main gate lead, this current flows through the forward biased bypass diode and prevents the occurrence of avalanche in the auxiliary cathode junction.

The feasibility and practicality of this approach was demonstrated on devices similar to those of this contract on a parallel Westinghouse program and later on by 35 thyristors that were purchased by NASA on Contract No. NAS 3-19097.

The second approach is to build the bypass diode in the silicon slice. This structure is shown in Figs. 5 and 6. As shown in Fig. 6, the diffused auxiliary cathode is segmented into two parts, A1 and A2. These parts function just like the standard amplifying gate—described in Section 3.2.1. Two bypass-diode diffused regions, B1 and B2, are formed at the same time as the diffusion of the main and auxiliary cathodes.

There are three features to be noted about the construction of this bypass diode. First, note that the metal overlaps the opposite side of the diffused region from that of the auxiliary cathodes. This clearly creates a diode polarity opposite of that of the auxiliary cathode. Second, there are small etch pits, E, between the segmented circular diffused regions. These etch pits prevent gate current from bypassing the auxiliary cathode during turn-on. Current that bypasses the auxiliary cathode is wasted and is not effective for fast, low loss turn-on. Third, there is an additional diffused layer or lip, which helps to prevent the bypass diode from refiring the device during the gate-assisted turn-off. This is sketched in Fig. 7.

The function of this lip diffusion is to cause the injection from the bypass diode to occur in an area in which the npn current gain is low so that it does not fire the thyristor. To understand the need for



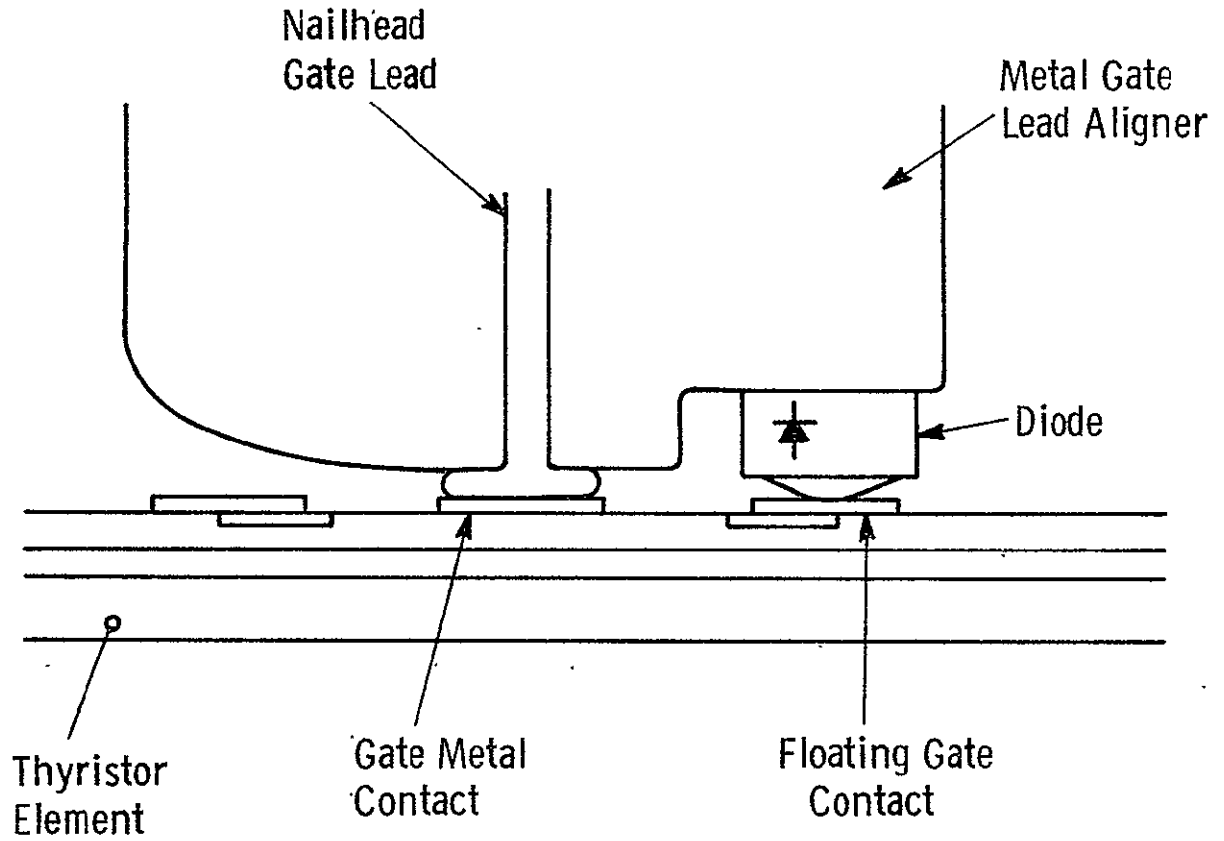
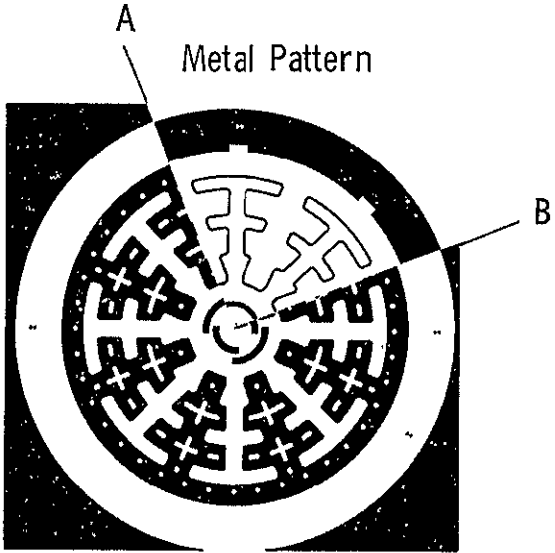


Fig. 4—Sketch of package modification with bypass diode



Diffused Cathode Pattern

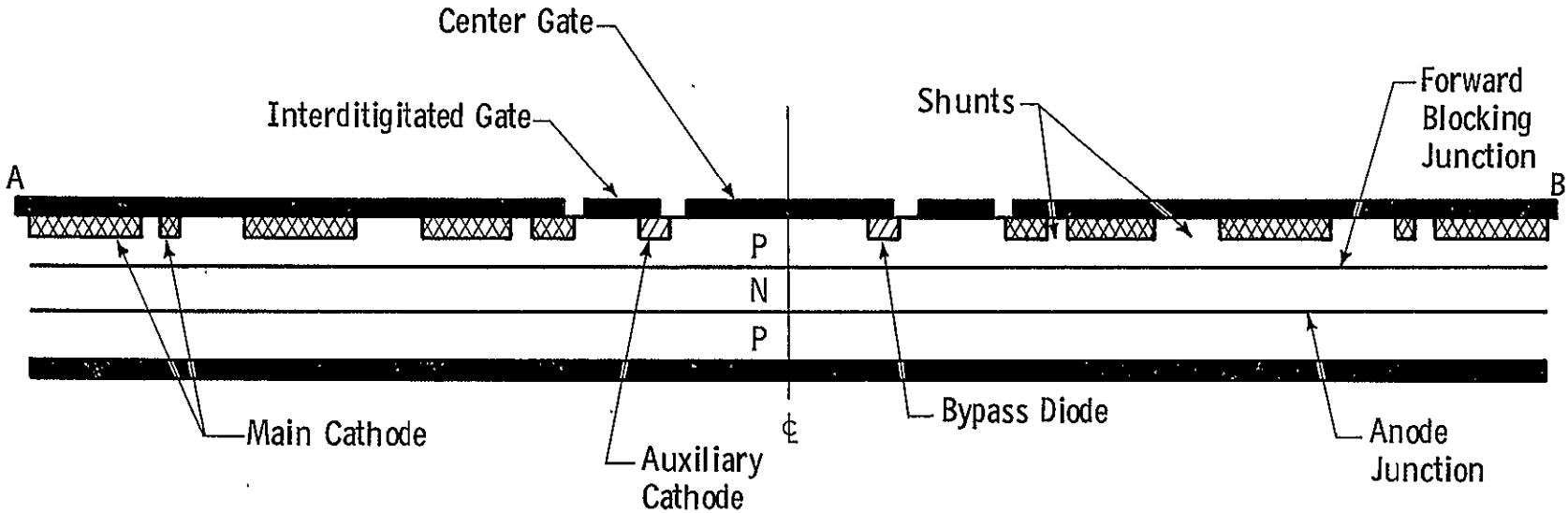


Figure 5—Thyristor structure with an integrated bypass diode

20

Dwg. 6292A37

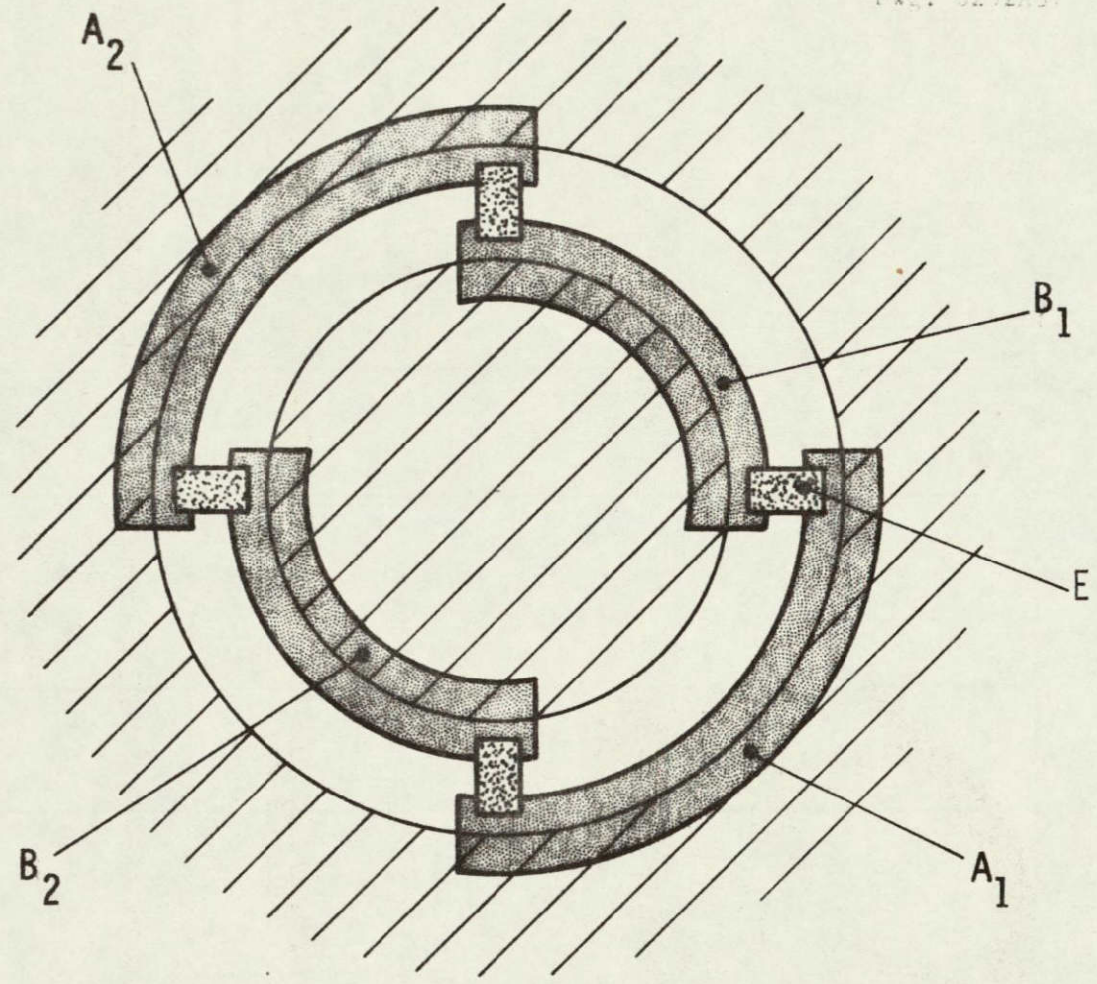


Fig. 6—Top view of gate having both gate amplification and a bypass diode

Dwg. 6252A87

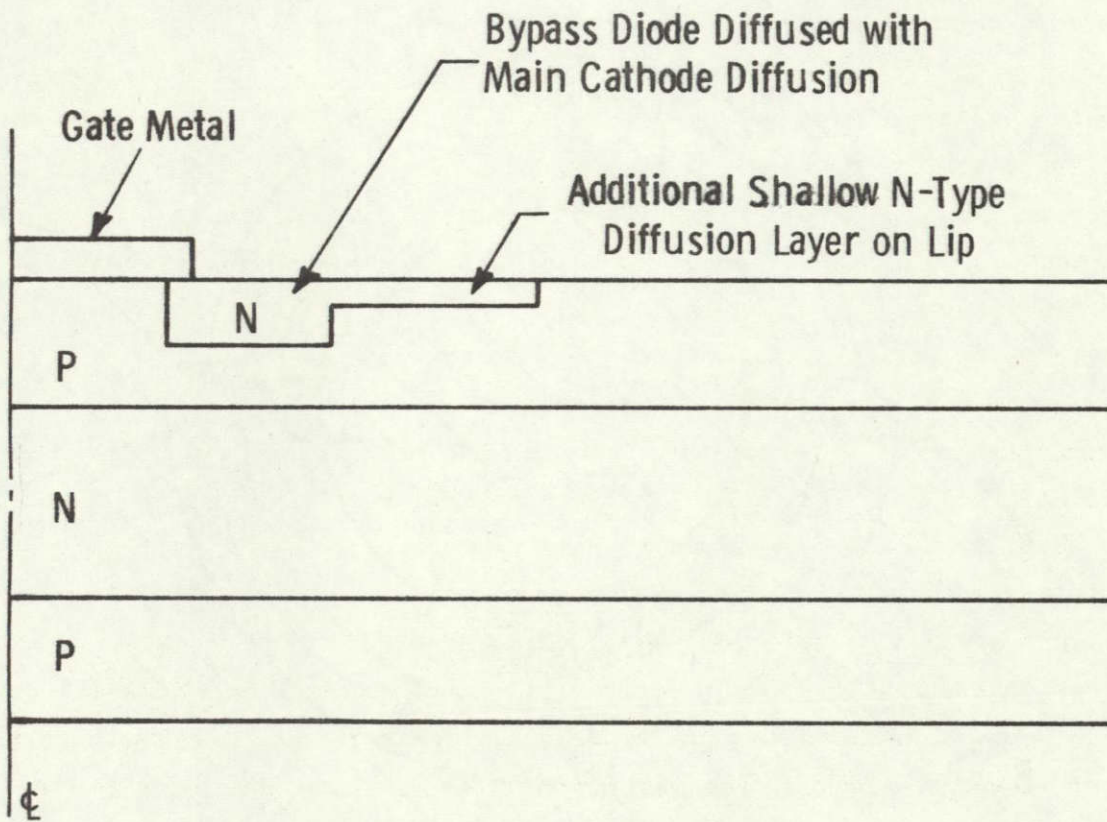


Fig. 7—Sketch of modification of integrated bypass diode to prevent injected electrons from firing the thyristor

this, consider what would happen if this npn current gain were not low. In this case, when current is drawn out the main gate, most of this current involves electrons being injected into the p-base. Many of these electrons reach the forward blocking junction and flow through to the n-base. These electrons are base current to the pnp transistor and partially turn it on. The impedance of the cathode circuit which is designed to carry several hundred amperes is lower than that of the gate circuit which was only designed to carry a few amperes. Therefore, the anode voltage of several hundred volts drives the current being carried by the pnp transistor mostly through the cathode. This current has the polarity to forward bias the cathode junction and fire the thyristor. To prevent the gate-assist current from firing the thyristor in this manner, a means had to be developed for minimizing the amount of gate-assist-current-induced electrons that reach the forward blocking junction. This was done by building the bypass diode in the form shown in Fig. 7. This design forces the injection of electrons from the bypass diode to occur over a larger area and an area in which the p-base width is wider. Such widening of the p-base width decreases the transport factor for electrons through the p-base and decreases the injection efficiency for electrons into the p-base.<sup>(5)</sup> The increase in the emitter area increases the amount of recombination that occurs in the space charge region of this bypass diode emitter—thereby further decreasing the injection efficiency for electrons. The injection efficiency and transport factor are both further reduced by area-selectively decreasing the lifetime under the extended bypass diode region.

### 3.2.5 Cathode Shape

The design implications of the physical model for turn-off which is described in Section 5 are:

1. Minimize the ratio of gate area to the peripheral length of the edge of the cathode.
2. Minimize the cathode line width.
3. Make shunts continuous lines with a minimum of corners.

A new device mask design has been prepared. Figure 8 shows a photograph of the cathode layer diffusion pattern.

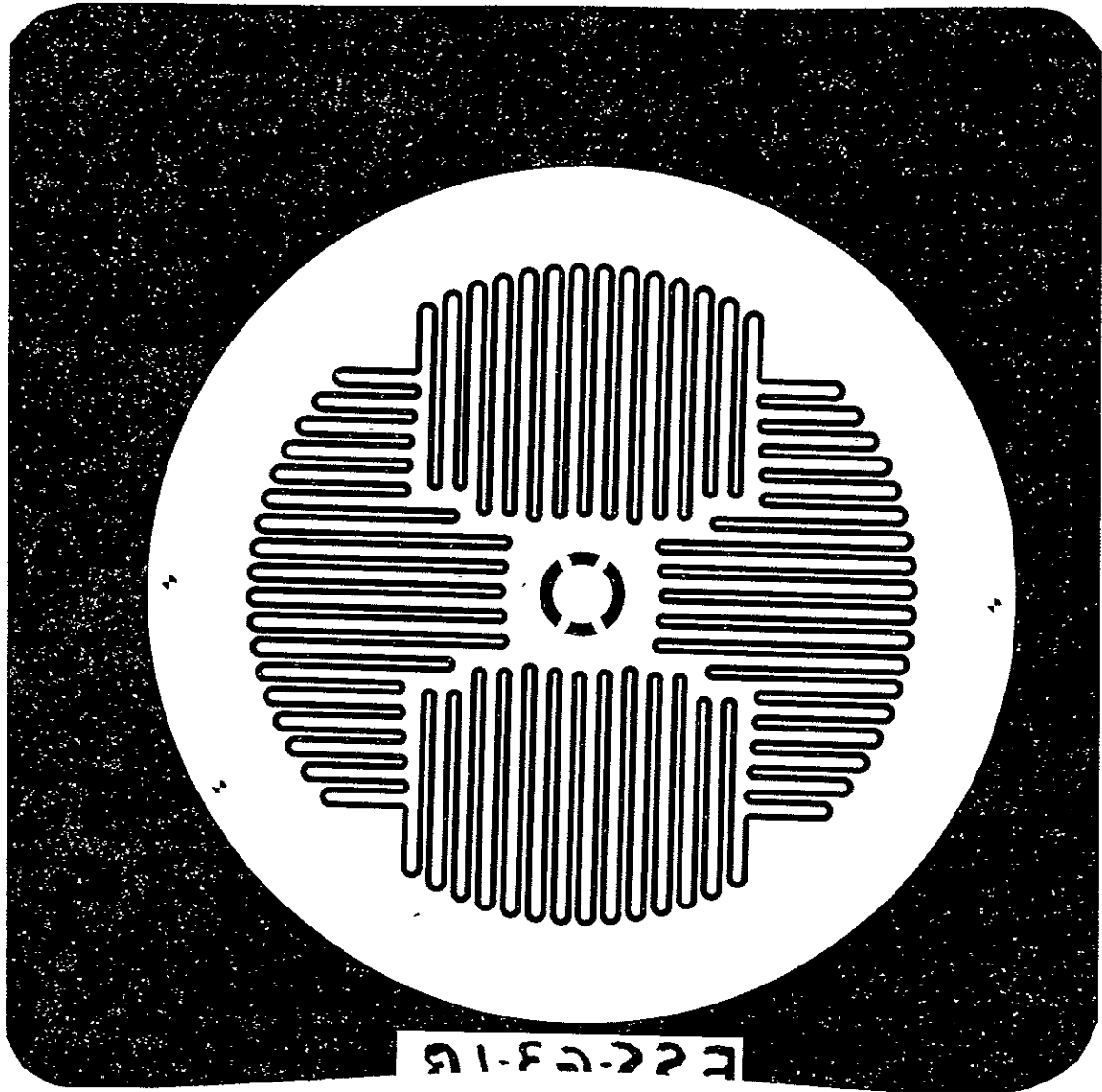


Fig. 8 - Photograph of cathode layer diffusion mask

#### 4. TEST CIRCUIT DEVELOPMENT

##### Introduction

All of the test circuitry used in this program was described with detailed circuit drawings on pages 29-60 of the final report of Contract NA53-14394, i.e., NASA report number CR-121161.

The two most important circuits used on the present contract are the turn-on circuit shown herein in Fig. 3 and the turn-off circuit shown in Fig. 9.

##### Turn-on Circuit

The turn-on circuit was shown in Fig. 3 herein and in more detail on pages 42 to 48 of NASA Report CR-121161. It consists of a pulse forming network that is charged up and then discharged through the thyristor under test. The anode voltage and anode current waveform are observed on an oscilloscope. Turn-on switching losses can be calculated from these waveforms.

Unfortunately, it seems to be a universal problem with this approach that one can never be sure that the voltage waveform is accurate because of the following:

- 1 If the anode voltage being switched from is as high as the normal operating voltage the pre-amplifier of the oscilloscope must be overdriven and saturated so that, at turn on, voltages of 0-5 volts can be read. This saturation of the preamplifier can produce erroneous readings. Sometimes this source of error is minimized by switching the thyristor on from a much lower voltage, say 30V. In this case, while the voltage



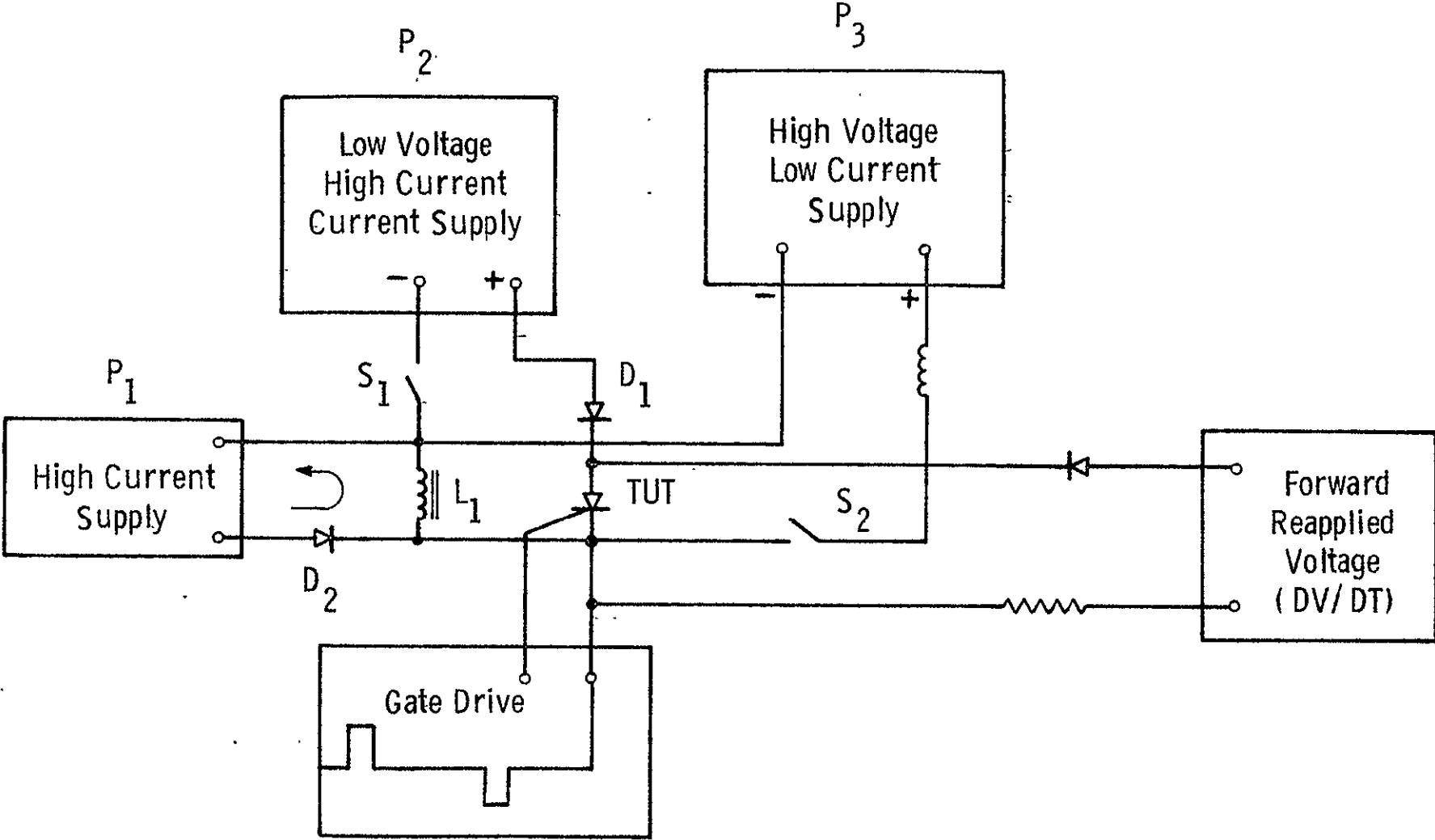


Fig. 9 - Turn-off time tester

waveform may be correctly measured, it may be significantly different from the one that occurs when the thyristor is switched on from a higher voltage in the circuit designers circuit.

2. In the environment of the device under test there are wires with very high  $di/dt$  and  $dv/dt$  levels. It is very difficult to be sure that either capacitive or inductive coupling has not influenced the voltage waveform that is measured. To overcome these uncertainties a new piece of equipment is being set up to measure energy losses in the thyristor. The heart of the new equipment is a calorimeter that will measure the heat generated in the thyristor being operated under conditions similar to those of the circuit on which it is to be used. Measurements are to be made with this equipment on the follow-on part of the program.

#### Turn-Off Circuit

Figure 9 is a block diagram of the turn-off test circuit. The operation of this circuit can be described as follows:

1. Initially power supply  $P_1$  creates a high current of say 200A in large inductance,  $L_1$ .
2. Next switch  $S_1$  is closed. This puts a forward voltage on the thyristor under test (TUT) so that TUT can be switched on with a positive gate signal. When TUT is switched on simultaneously with  $S_1$ , the voltage from  $P_2$  reverse biasses  $D_2$  and diverts the 200A in  $L_1$  through TUT.

3. Next TUT is commutated off by closing switch  $S_2$ . This puts a relatively high reverse voltage on the loop containing  $L_1$  in parallel with TUT,  $D_1$  and  $P_2$  and causes a linear decrease in current through TUT of say 25A/ $\mu$ sec. This continues until the current through TUT has been reduced to zero, and reverse recovery has occurred on TUT.
4. Next a forward voltage  $dv/dt$  ramp is reapplied to TUT. The duration of the interval between when the anode current was commutated through zero and when forward voltage is reapplied is the turn-off time. This duration is varied to find the minimum time for which TUT can support forward voltage and this is recorded as the turn-off time for that device.

The gate drive circuit creates a forward gate pulse to turn TUT on and at an adjustable time later a reverse gate current can be applied to the gate. This reverse current is the gate assist current. The time of initiation and the pulse height and width of this reverse gate current are adjustable.

It is very important that the reverse recovery time of diode  $D_1$  be matched to that of TUT. If diode  $D_1$  recovers too soon, it prevents the reverse current from sweeping out all of the sweepable excess charge from TUT. (Not all excess charge is swept from TUT even when TUT reverse recovers but it is important that as much charge be swept out of TUT before it reaches reverse recovery, i.e., it is important that diode  $D_1$  doesn't limit excess charge sweepout from TUT.)

## 5. . PHYSICAL MODEL FOR THYRISTOR TURN-OFF

### 5.1 Introduction

Based on extensive theoretical and experimental work, a comprehensive model has been developed. This model provides the basis for understanding a broad range of thyristor turn-off related phenomena, covering the behavior and interaction of the turn-off time, reverse and forward recovery currents and the allowable  $dV/dt$  rating. The model provides an excellent basis for designing thyristors for a fast turn-off either in the gate-assist (but not gate-controlled) or non-gate-assist model.

The description of the model will be best understood if the reader understands how all thyristors involved in commutated turn-off go through the following sequential steps:

- A device in conduction
- Current commutation
- Current polarity reversal
- Reverse recovery
- Forward voltage reapplied ( $dV/dt$ )
- Forward-recovery-current induced IR drop
- IR drop causes cathode injection and fires the thyristor

The effect of a gate-assist current is described in the following two models:

Earlier Model - carrier sweep out

Present Model - counteracting voltage on p-base

### 5.2 Thyristors in General

#### 5.2.1 A Device in Conduction

Starting with a thyristor in the conducting state that is to be turned off, it is important to understand that the anode emitter is

emitting holes over its entire area. This is the result of the high density of acceptor atoms in the anode layer and of the high (modulated) conductivity in the n-base layer which make both layers nearly equipotentials. This uniform injection creates an excess hole density and, because the region is space charge neutral, an excess electron density that is fairly uniform over the entire area of the n-base. This is illustrated in Fig. 10. (Experimental evidence in support of this is given on page 57.)

#### 5.2.2 Current Commutation

While the anode current is being commutated toward zero, the injection levels from both the cathode and the anode emitters are decreased. This decreases the excess charge density both because of a carrier flow from the p- and n-bases and because of recombination. Figure 11 illustrates this.

#### 5.2.3 Current Polarity Reversal

When the anode current is reversed, the emitters stop injecting. Excess charge continues to flow out, as shown in Fig. 12, and recombination continues to take place in the p- and n-bases.

#### 5.2.4 Reverse Recovery

Later when the excess charge densities are decreased to zero at the anode junction, the current-carrying capability of the anode junction drops abruptly and the device "blocks," i.e., supports voltage. This is reverse recovery. At this stage of turn-off, the anode junction limits the current to a sharply reduced value. The voltage polarity on this junction prevents electrons from leaving the n-base through the anode junction. On the other side of the n-base, at the central junction, the dopant density distributions are such that this junction injects holes from the p-base in much greater number than it injects electrons from the n-base. Therefore, only a small proportion of the already small anode-junction-limited current consists of electrons leaving the n-base in the direction of the p-base. Clearly, after reverse recovery, the flow of excess electrons from the n-base is nearly

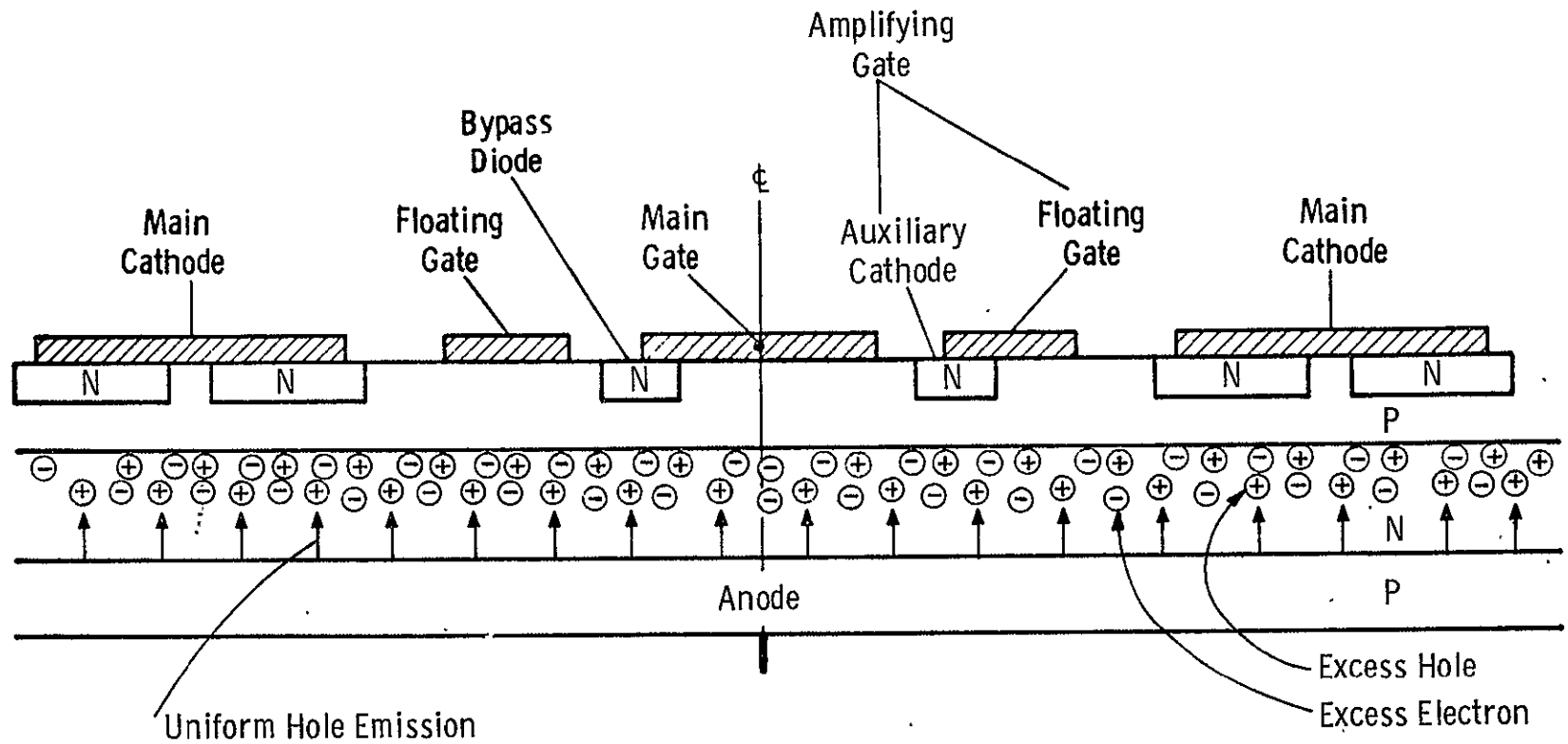


Fig. 10—Model of thyristor in conduction. Thyristor in on-state has uniform emission of holes from anode into N-base throughout the anode area. (The injection of electrons from the cathode emitter is not shown to improve the clarity of the sketch).

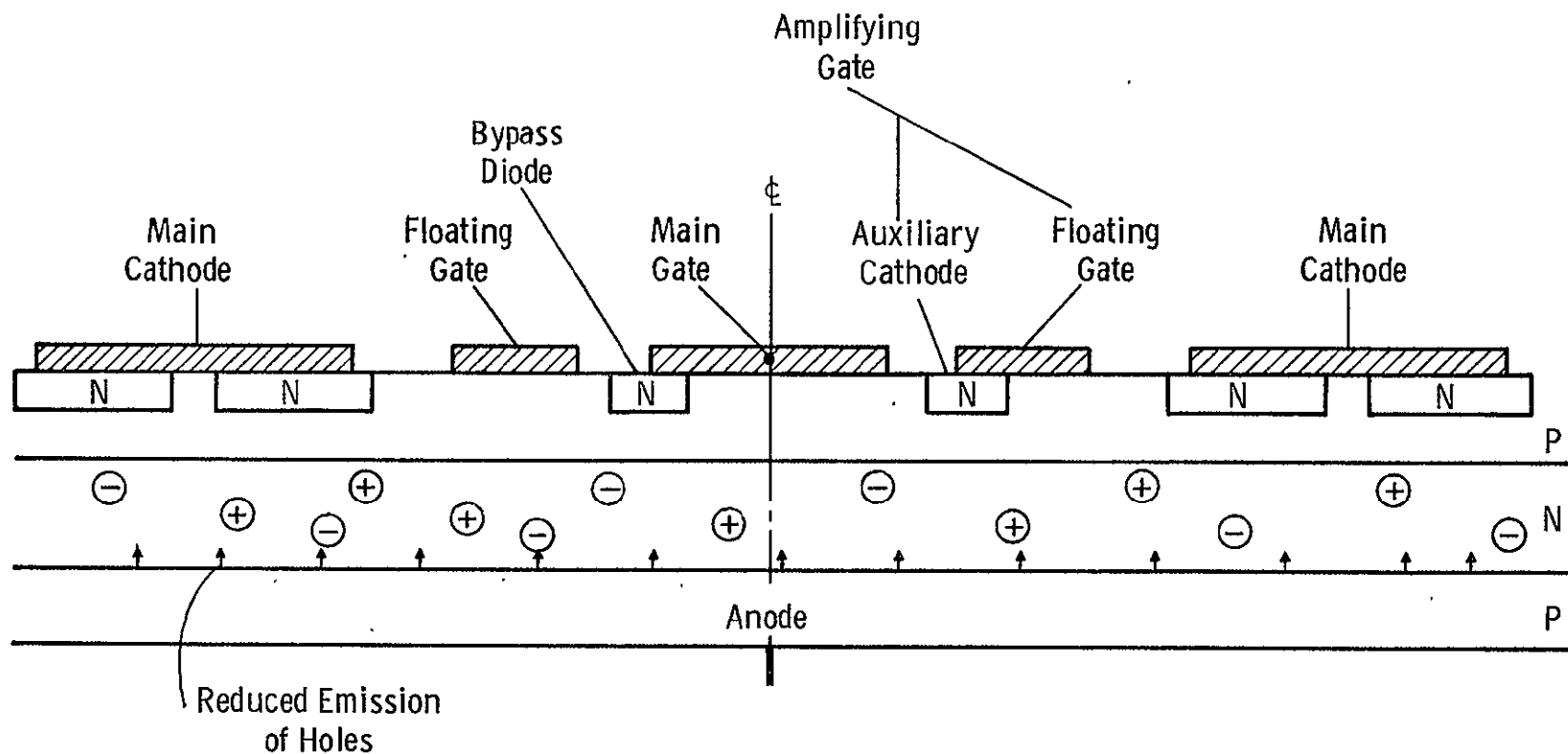


Fig. 11—Model of thyristor being commutated. While the anode current is being commutated toward zero, the injection levels and excess charge density are decreased.

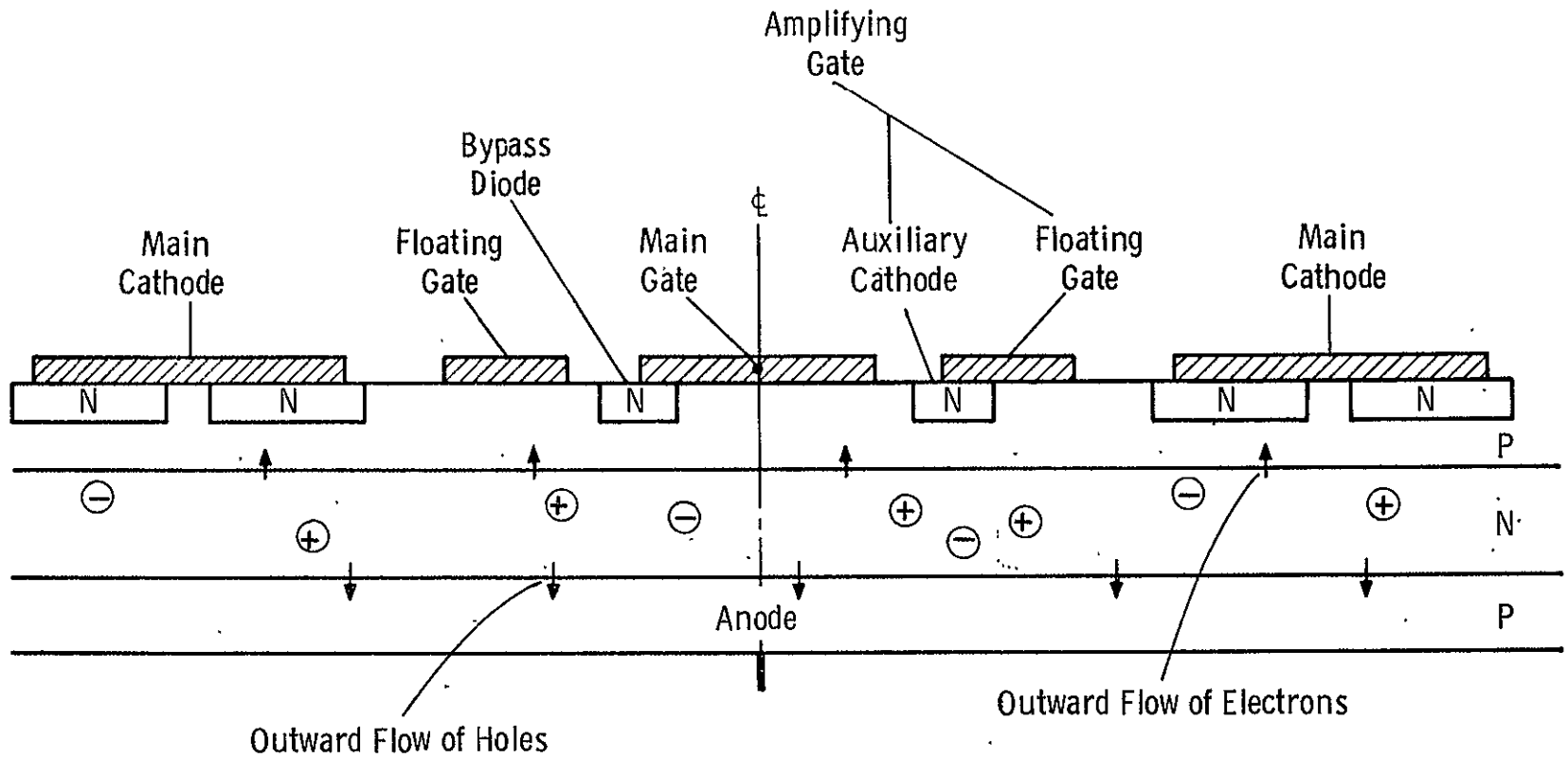


Fig. 12 — Model of thyristor with reverse current, After the anode current has commutated to a reversed polarity, carrier injection stops and some excess carriers flow out.



stopped at both junctions. This is illustrated in Fig. 13. An equal number of excess holes is present to neutralize the charge of these electrons to maintain space charge neutrality. Assalit and Studtmann<sup>(6)</sup> reported that turn-off time can be decreased by means of a current in a lead attached to the n-base. This is additional evidence that the model for thyristor turn-off is valid; but the use of an n-base gate lead is undesirable because it complicates the manufacturing process and the circuit design.

For thoroughness, one should consider whether the design of the cathode junction (i.e., whether it is shunted and what is its avalanche voltage) affects this phase of the operation. The cathode junction design is not important in this stage of turn-off. Whether it is shunted or not will most likely determine whether the reverse voltage avalanches the emitter junction. But even if the cathode junction is avalanched, the anode junction limits the current to a sufficiently low value that the holes generated by the avalanche will not significantly affect charge densities in the p- or the n-base.

#### 5.2.5 Forward Voltage Reapplied (dV/dt)

The next phase of turn-off occurs when forward anode voltage is reapplied. The anode junction again becomes conductive and electrons can flow out the anode junction. As electrons flow out to the anode, the requirement of space charge neutrality allows holes to flow out to the p-base and on out through the cathode shunts, as shown in Fig. 14. This current continues until the excess charge at the central junction is reduced to zero, and then forward recovery<sup>(7)</sup> occurs at the central junction in a manner very similar to that of reverse recovery. This is depicted in Fig. 15.

It should be noted that if the device is being subjected to a fast rising forward voltage pulse, even when there is no excess charge, there is a small pulse of current because of the need to remove charge to create the depletion layer that supports the voltage. Another way of saying this is that the transition capacitance must be charged. If the dV/dt is high enough, this current causes dV/dt firing of the device even if there was no excess charge.

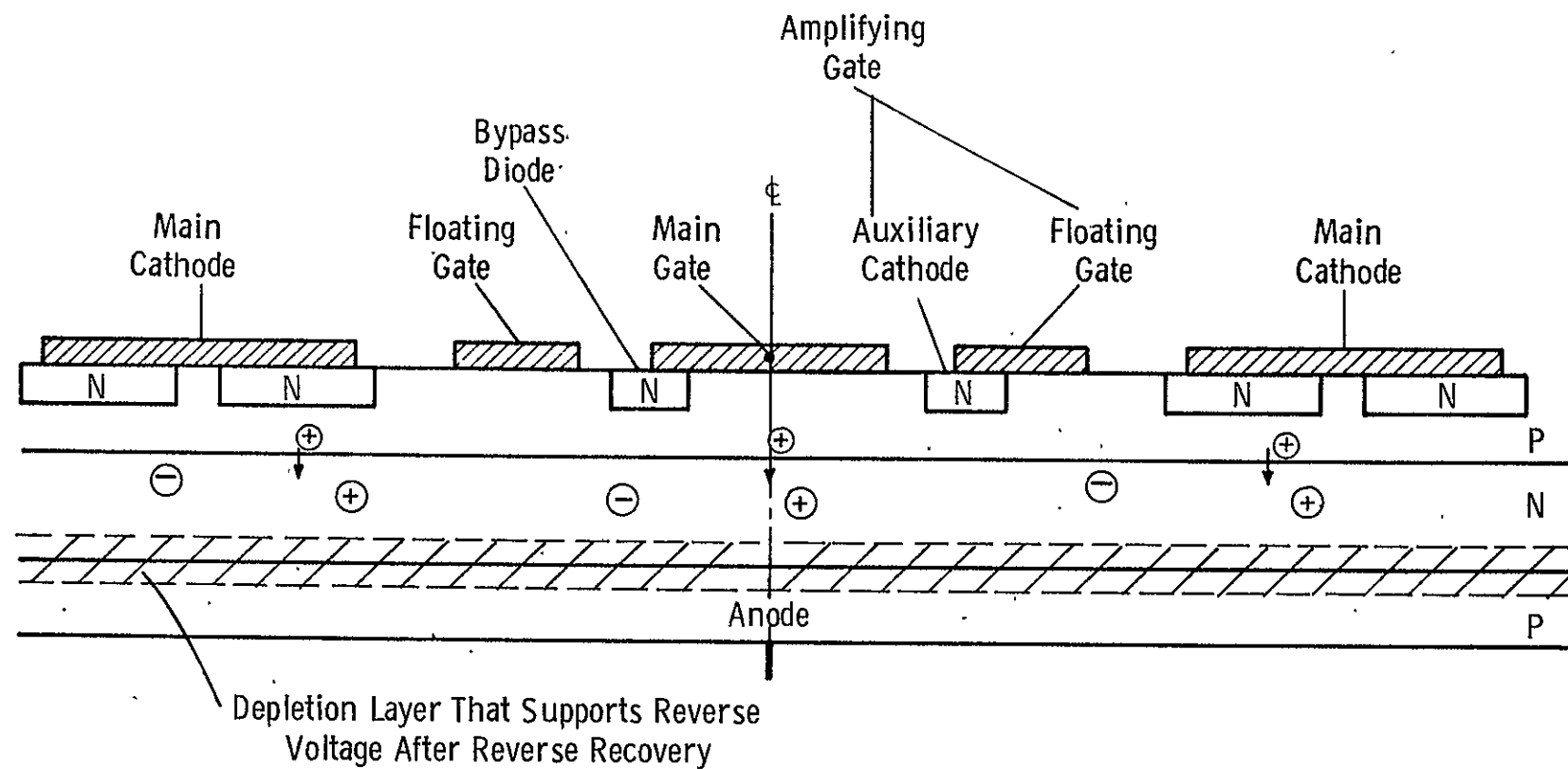


Fig. 13—Model of thyristor at reverse recovery. At reverse recovery the excess charge density at the anode junction has decreased to zero. The junction develops a depletion layer and supports voltage. Excess charge remains in the N-base. The central junction carries a very low current consisting mainly of holes flowing into the N-base.

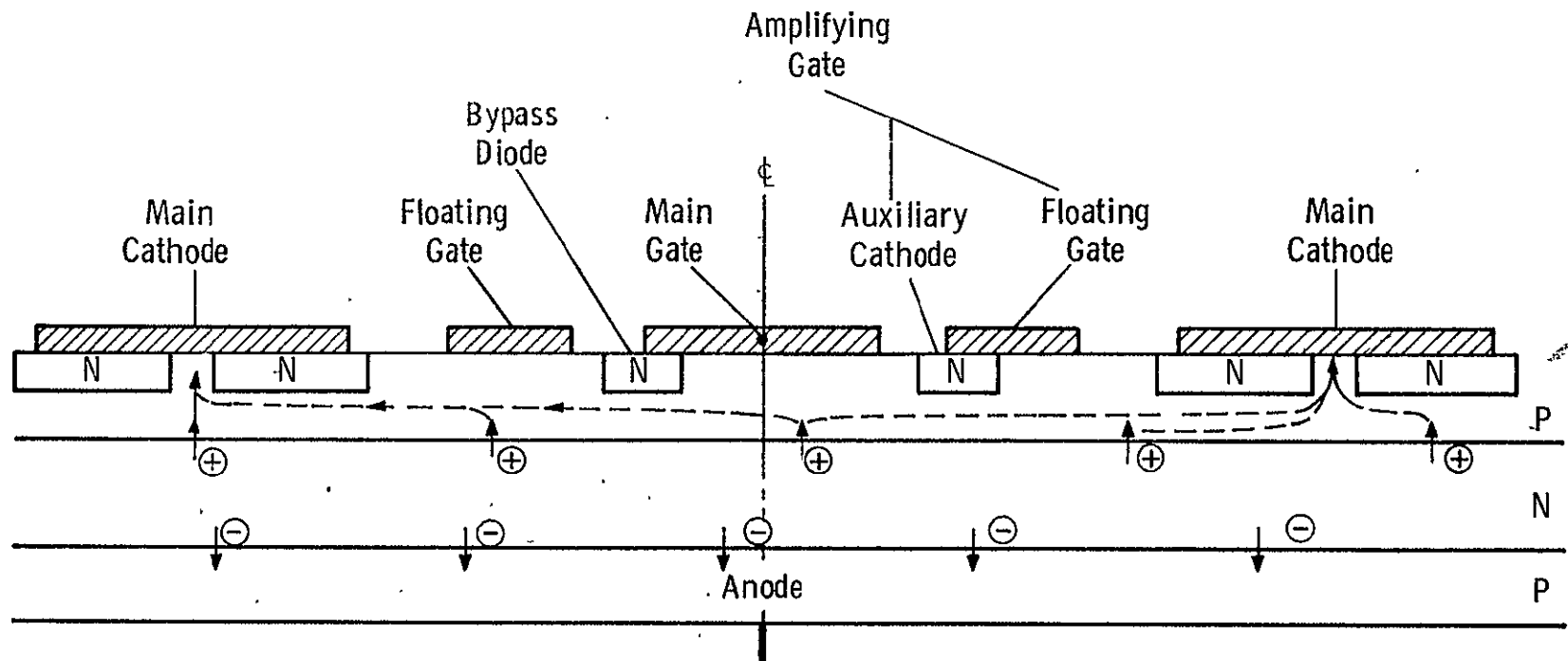


Fig. 14—Model of thyristor when forward voltage is reapplied; When forward voltage is reapplied, excess electrons can flow out through the anode junction and excess holes can flow out through the center junction. The holes are majority carriers in the P-base and carry current out through the cathode shunts.

38

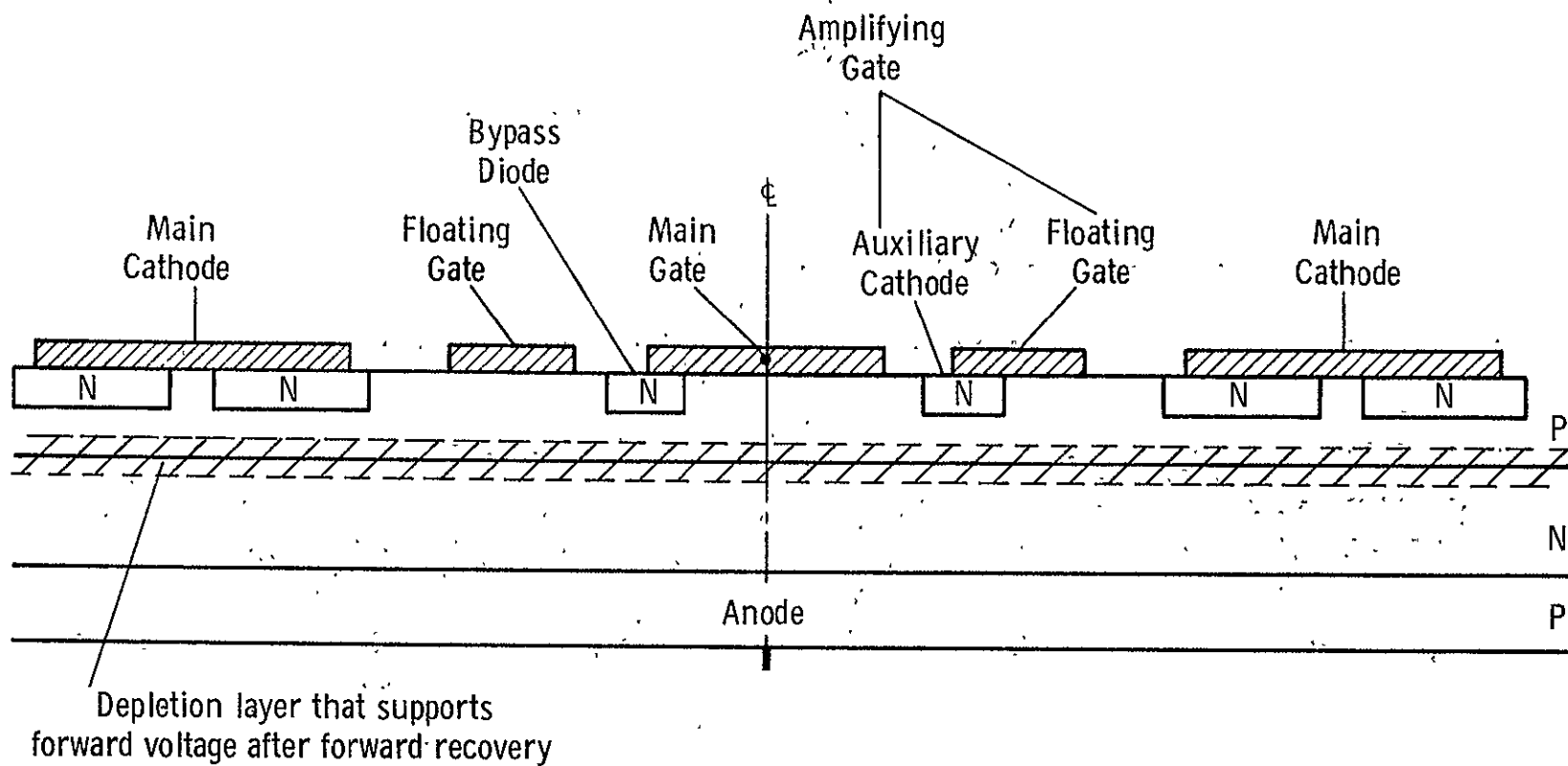


Fig. 15—Model of thyristor at forward recovery. Forward recovery occurs when the excess charge density at the central junction has decreased to zero. A depletion layer forms at the central junction which blocks current flow and supports the reapplied forward voltage.

Again, one should ask whether the cathode design affects the turn-off behavior -- this time the forward recovery current. It is conceivable that the cathode emitter might be injecting electrons during the forward recovery phase that add to the forward recovery current. If this were significant, shunting the cathode would reduce such injection, and this might reduce the forward recovery current and the turn-off time. The evaluation of the significance of this is beyond the scope of this contract.

#### 5.2.6 Forward Recovery-Current-Induced IR Drop

The turn-off time and the  $dV/dt$  rating depend on the forward recovery current as follows. The forward recovery current enters the p-base over the entire area of the middle junction and flows to, and out through, the cathode shunts. This current develops a voltage drop across the lateral resistance of the p-base as shown in Fig. 16. The magnitude of this voltage drop depends on:

1. The magnitude of the forward recovery current.
2. The lateral resistance in the p-base to this current.
3. Device geometrical factors that determine the current path distribution in the p-base.

The variables that determine (1) were described above; the variables that affect (2) are:

- a. The diffusion layer profiles of both the p-base and the n-type cathode emitter.
- b. The geometry of the emitter diffusion mask including such things as the cathode shunt pattern, emitter line width, and the ratio of gate area to cathode edge length.

Concerning (3), the resistance is not a simple one in which current enters in one end and leaves out the other. Charge flows into the p-base all over its area and then flows laterally toward the cathode shunts.

40

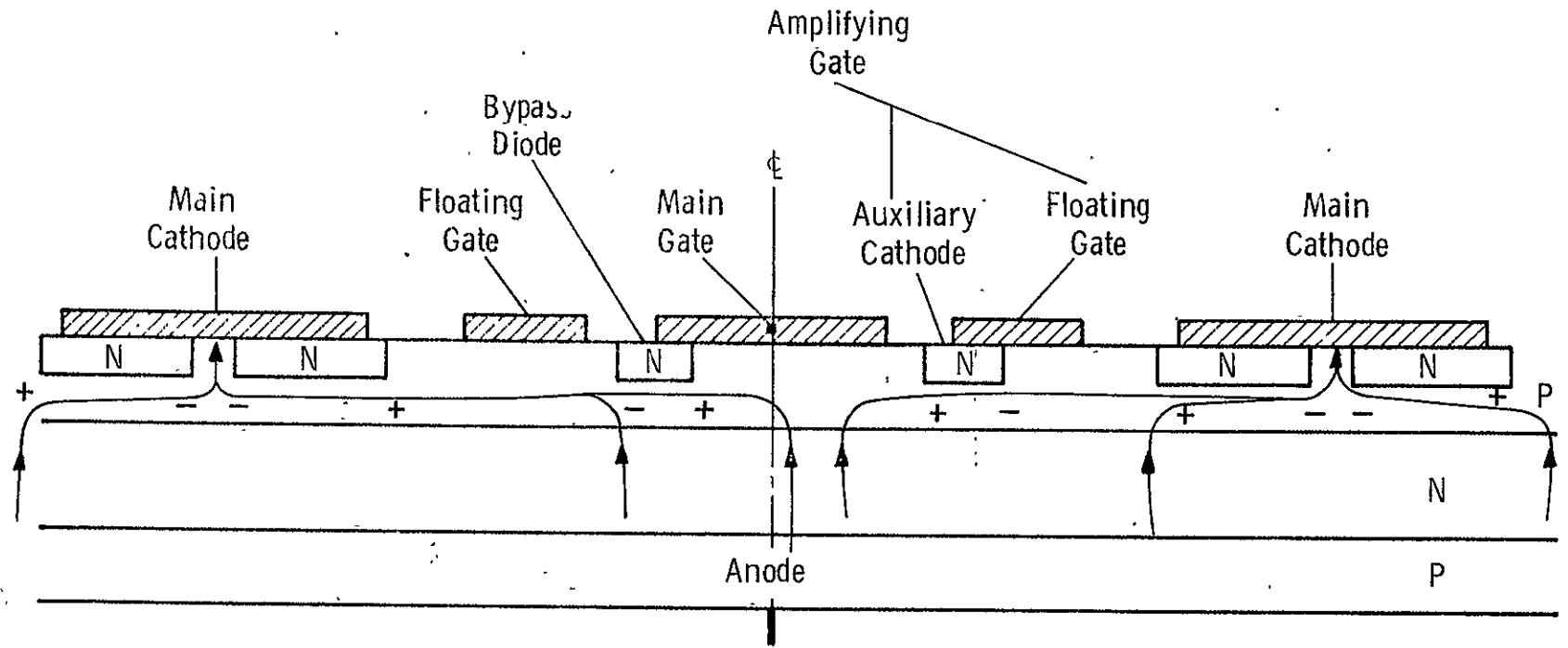


Fig. 16—Model of thyristor with forward-recovery-current-induced IR drops in P-base; Forward recovery current creates an IR drop in P-base under the cathodes that forward biases the cathode emitters.

### 5.2.7 IR Drop Causes Cathode Injection and Fires the Thyristor

If the IR drop in the p-base due to the forward recovery current is greater than about 0.7V, it forward biases the cathode emitter as shown in Fig. 17. If this cathode emission continues long enough, the injected carriers diffuse through the thyristor bases and build up a sufficient density distribution of excess carriers to refire the thyristor. This is described in Fig. 18.

Because the time it takes to build up the carrier distribution (about a microsecond) depends on the injected carrier density, the IR drop that is capable of refiring the thyristor depends on the duration of the forward recovery current pulse which, in turn, depends on the  $dV/dt$  applied to the anode.

Figure 19 shows how the peak forward recovery current needed to refire a thyristor increases with increasing  $dV/dt$ . The time interval between the onset of forward-voltage-induced displacement current and the forward recovery point (at the current peak) decreases with increasing  $dV/dt$ . It is this leading portion of the forward recovery pulse that determines whether the device refires.

Of course, the diffusion layer profiles and the n-base width, the resistivity and the lifetime all influence the current gains of the npn and the pnp transistors in the two transistor analog. These design variables, therefore, all influence the forward-recovery-current-induced IR drop that refires the device.

## 5.3 Gate-Assisted Turn-Off

### 5.3.1 Carrier Sweep Out Model

At the start of the program, it was generally believed that the function of gate-assist current is to sweep out the excess carriers through the gate and, thereby, reduce the turn-off time by reducing the amount of carriers that must recombine before a forward voltage can be

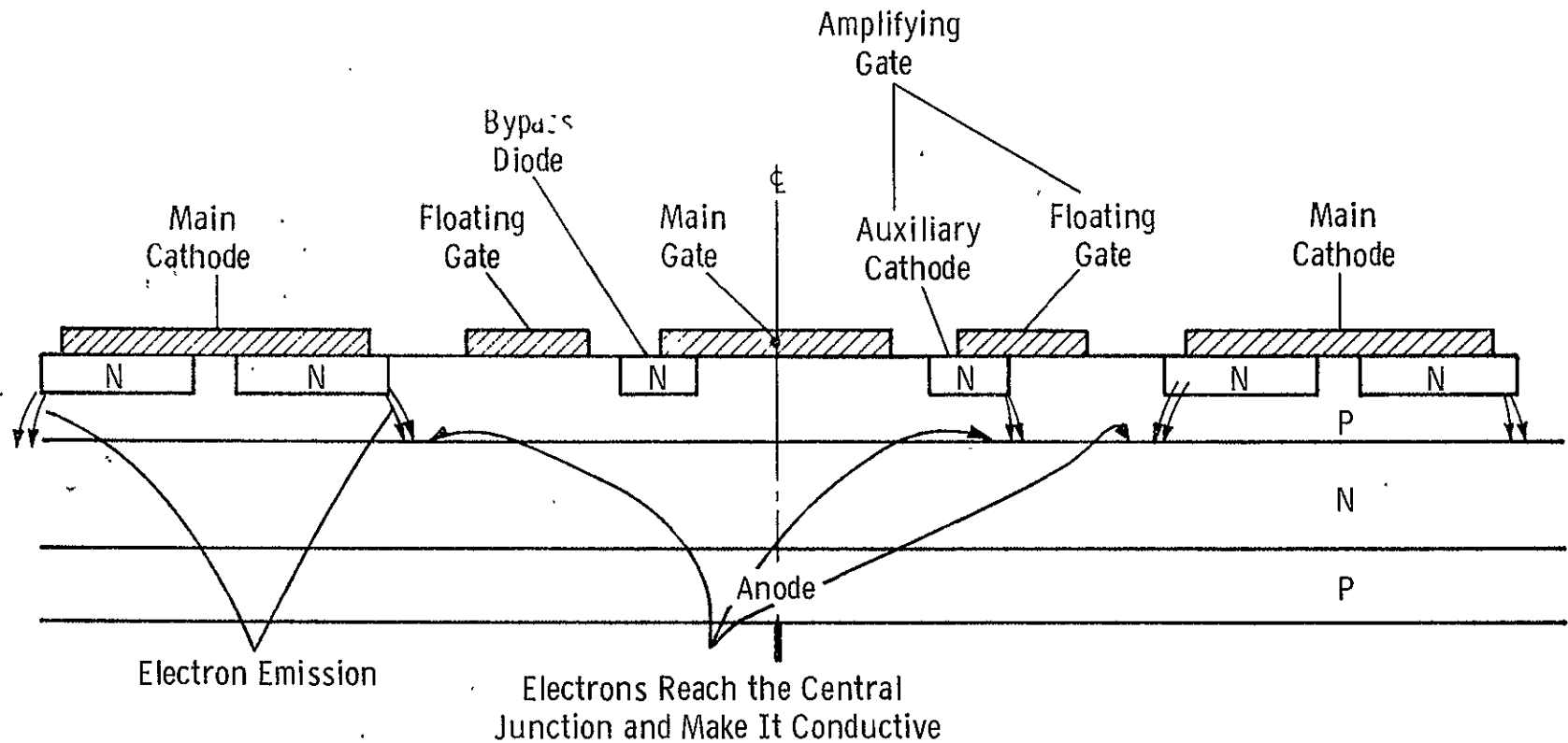


Fig. 17—Model of thyristor when the IR drops in P-base cause cathode emission. If the magnitude and duration of the forward recovery current are sufficiently large, electrons will be emitted from the cathode that diffuse to the central junction and make it conductive.



43

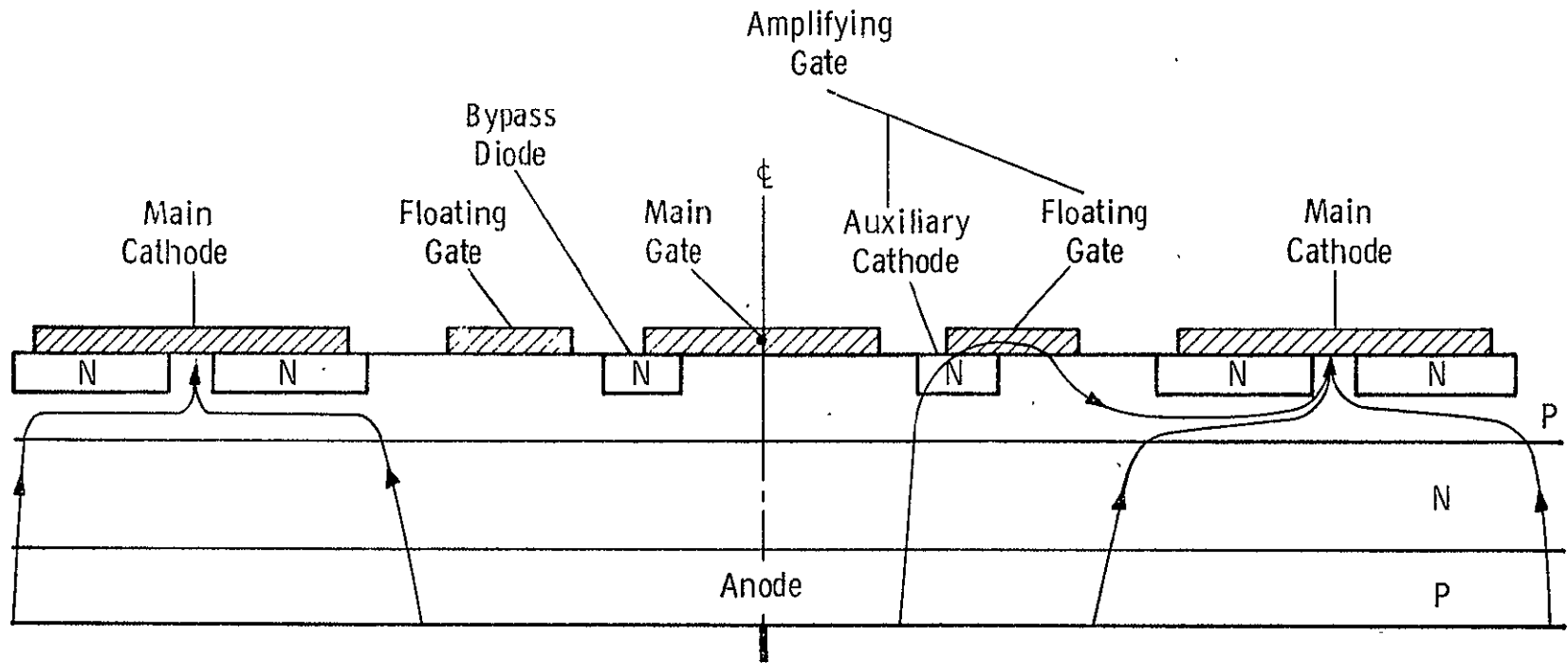
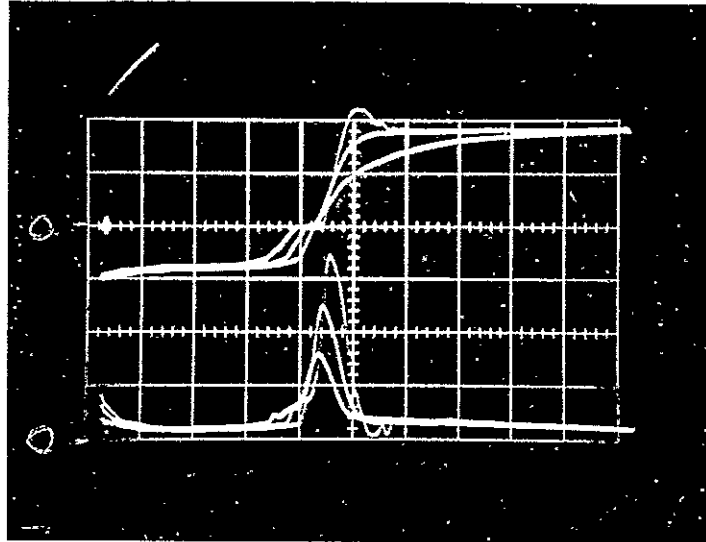


Fig. 18—Model of thyristor at refiring. The conductive central junction permits current to flow from the anode to the cathode. This increases the IR drop under the cathode and forward biases the cathode harder. As the currents rise, the alphas rise, and if the sum of the alphas reaches unity, the device fires.



Top: anode voltage (200 V/div)  
 Bottom: anode current (2 A/div)  
 time (1  $\mu$ sec/div)  
 temp. 100°C

Fig. 19. The effect of the  $\frac{dV}{dt}$  on the forward recovery current pulse height and pulse sharpness

Each set of curves was photographed just at the point at which a shorter turn-off time interval would re-fire the thyristor.

The "ledge" in the voltage ramps are due to an inability of the circuit to maintain the voltage ramp during the forward recovery current pulse.

reapplied as depicted in Fig. 20. In the course of the work on this contract, it was demonstrated that carrier sweep out is a fairly insignificant effect. This was done by showing that gate-assist current before the forward voltage ramp is reapplied is hardly effective for decreasing the turn-off time on the forward recovery current. For example, Fig. 21 shows that a gate-assist current applied in the interval between where the anode current has been commutated to zero and where the forward voltage is reapplied has little effect on the forward recovery current. Since it does not affect the forward recovery current, it should not affect the turn-off time. This has been experimentally verified many times.

This demonstration, that gate-assist current, applied before the forward voltage is reapplied, does not affect the forward recovery current, is direct evidence that not much charge is swept out.

### 5.3.2 Counteracting Voltage on p-Base

The effectiveness of the gate-assist current is primarily due to its creating a voltage drop in the lateral resistance ( $R_p$ ) of the p-base that counteracts a similar but oppositely polarized voltage drop due to the forward recovery current. Figure 22 illustrates this counteracting effect. This prevents, for a given  $dV/dt$  and forward recovery current, the build-up of an  $IR_p$  drop of sufficient magnitude to fire the devices. This permits the  $dV/dt$  to be increased and/or the turn-off time to be reduced.

Once it is understood that the effect of gate-assist current is to counteract the effect of forward recovery current, it is evident that a better understanding of the effects of differing operating conditions on forward recovery current is called for. Such understanding was developed in a study during this program that resulted in the paper of Ref. 7.

It is important to recognize that the objective with gate-assist current is not to merely reduce the forward-recovery-current-induced  $IR_p$  drop under the cathode. Fundamentally, the objective is to prevent this

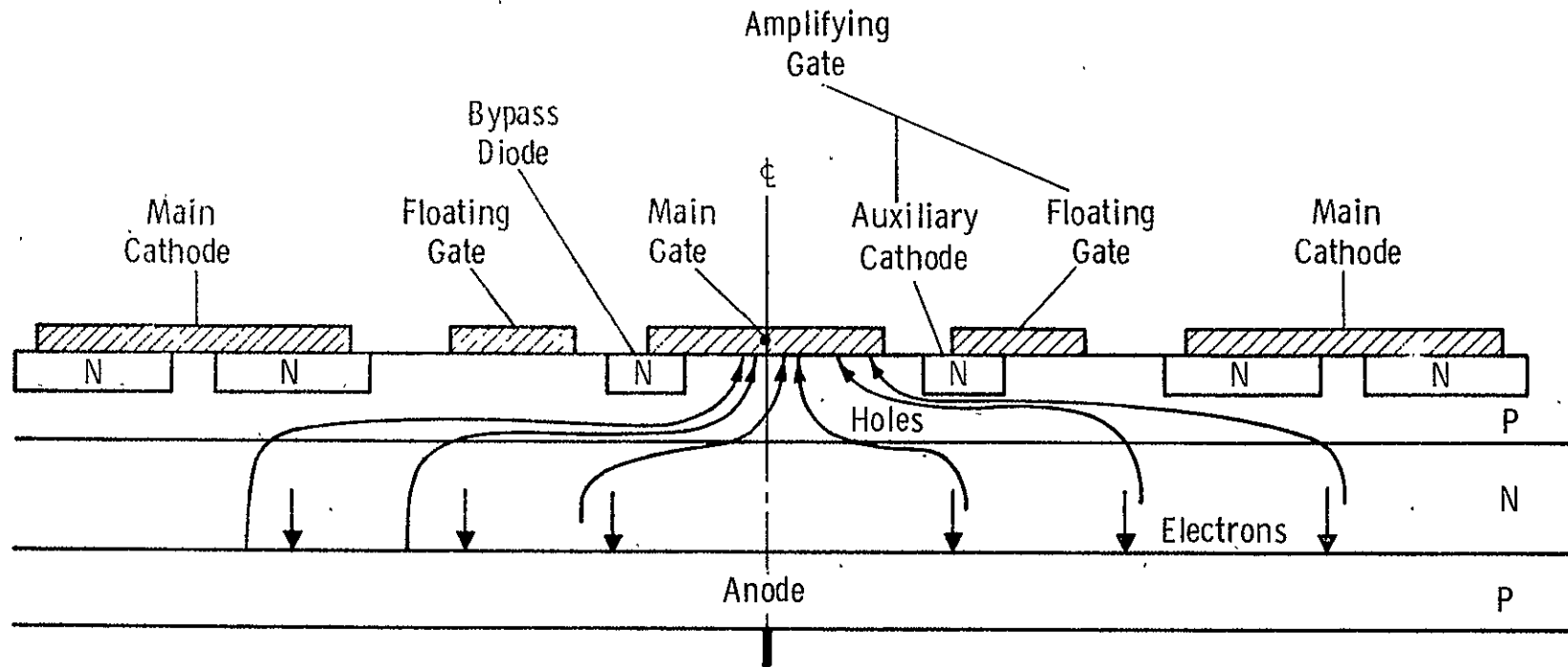
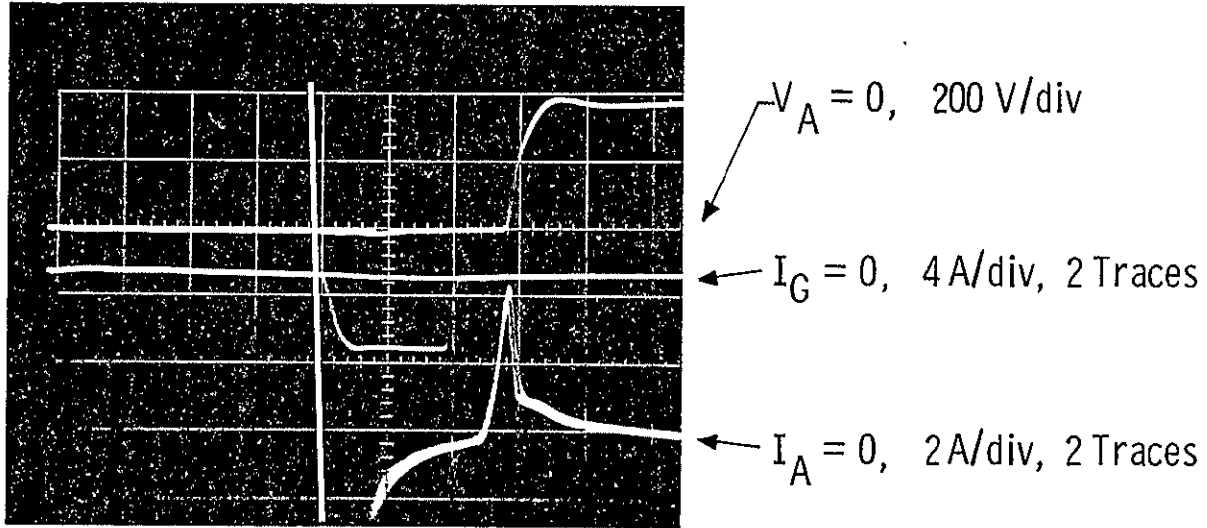


Fig. 20—Earlier model for gate assist. Earlier model—excess carriers were believed to be swept out by the gate assist current.



$2 \mu \text{ sec/div}$

$$I_{TM} = 200 \text{ A}, \frac{di}{dt} = 25 \text{ A}/\mu \text{ sec}, 100^\circ \text{C T-7}$$

Fig.21 - Gate-assist current removes little excess charge

48

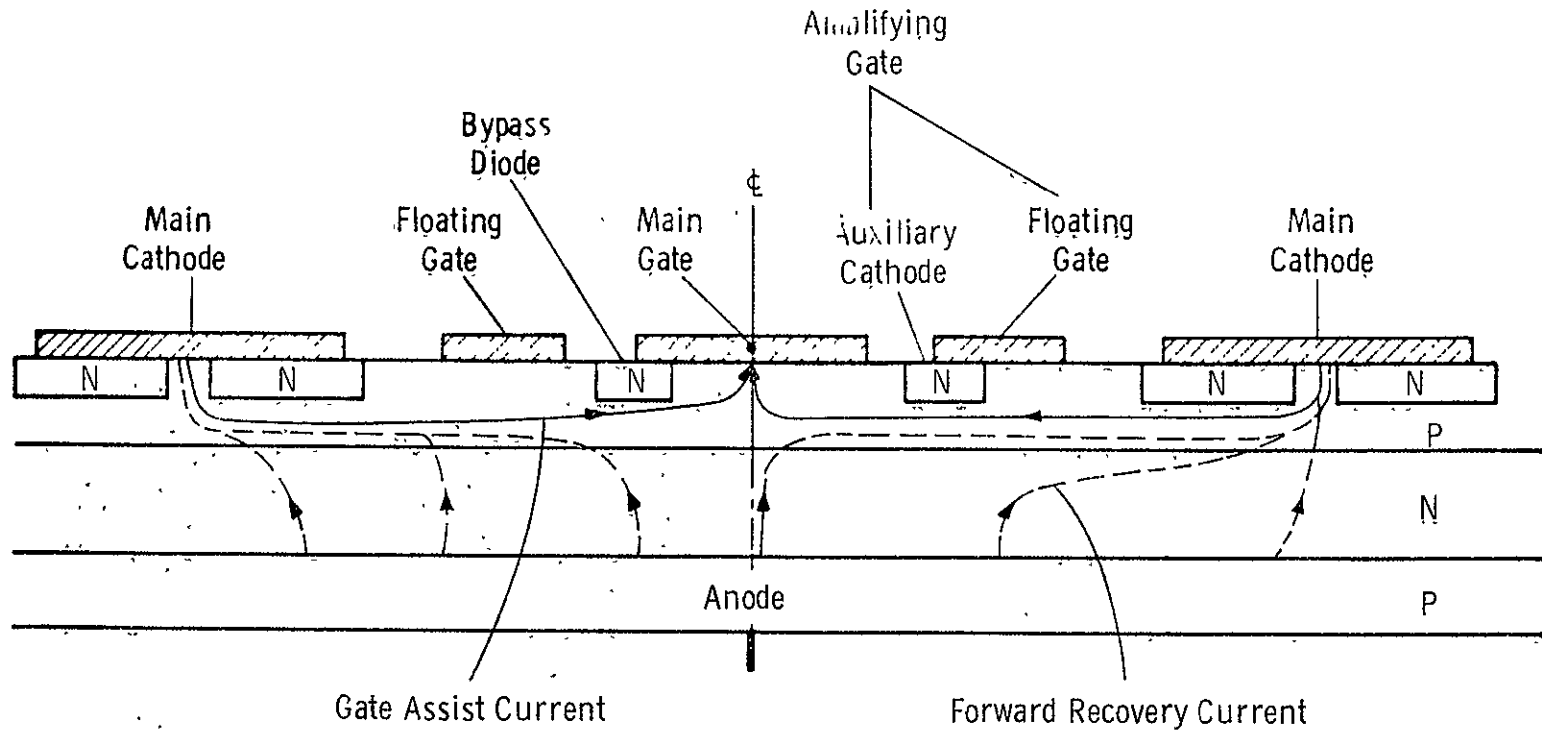


Fig. 22 —Improved model for gate assist. Gate assist current is effective because it provides an IR drop that opposes the IR drop generated by the forward recovery current.

$IR_p$  drop from exceeding a value of roughly 0.7V. For a given gate-assist current (e.g., 2 amperes), its effectiveness for counteracting the  $IR_p$  drop increases as the resistance increases. If this resistance is decreased, with everything else unchanged, the turn-off time, without gate assist, would be decreased but the gate assist current would be less effective.

To increase the effectiveness of gate-assist current, this lateral resistance of the p-base must be increased. However, when this is done, the current through this lateral resistance must be decreased by changing the cathode-gate geometry and by decreasing the carrier lifetime.

#### 5.4 Related Considerations

While this physical model is very useful for explaining turn-off, both reverse and forward recovery, and  $dV/dt$  behavior qualitatively, it must be recognized that a number of other factors significantly affect these parameters.

An increase in temperature will increase  $t_q$  and  $I_{RR}$  and decrease the  $dV/dt$  rating. The level of current being switched off will usually not affect  $t_q$  or  $I_{RR}$  because the time required to commutate the current to zero is at least several carrier lifetimes long. Increasing the rate at which the current is commutated to zero will increase  $I_{RR}$  and  $Q_{RR}$  and will possibly increase  $t_q$ .

The effects of the reapplied forward  $dV/dt$  were described earlier. The effect of the voltage level reached by the  $dV/dt$  ramp is not significant.

In addition to these variables, which should always be given when a  $t_q$ ,  $I_{RR}$  or  $dV/dt$  are specified or reported, there are significant factors that are rarely mentioned. These include:

1. The impedance of the gate circuit --if it influences the actual gate current that flows during the switching transient period.

2. The limiting resistance in the part of the test circuit that generates the  $dV/dt$  ramp because this can limit the forward recovery current.
3. The degree to which the recovery times of diodes and/or thyristors in the test circuit match the recovery time of the thyristor under test. If a component in the test circuit has reverse recovery too early, that component will interrupt the sweep out of the excess charge from the device under test. On the other hand, if it takes the component of the test circuit too long to recover, the test circuit cannot reapply a forward voltage on the device under test as soon as it is capable of supporting a reapplied forward voltage. In the first case, the device under test is not permitted to turn-off as fast as it might if more excess charge were swept out. In the second case, the circuit will not be able to measure the true turn-off time.
4. Any inductance in the leads to an anti-parallel diode. Such inductance can force a forward current into the thyristor under test during the turn-off time interval. This unwanted forward pulse is diverted into the device under test when reverse recovery occurs in the diode that isolates the lower impedance current generating circuitry from the high impedance voltage generating circuitry.
5. The width and shape of the anode current pulse because this determines whether the device is carrying the current uniformly over its area.



6. The shape of the reverse voltage waveform because this influences the amount of charge that is swept out of the device in the reverse recovery phase. The rate of application of this voltage is believed to be more important than the ultimate voltage reached.

## 6. DEVICE FABRICATION

At the start of the program, devices were being made both at the Research and Development Center and at the manufacturing division. In each case, the process most suited for these devices in use at that location was chosen.

Both processes can be described by the flow chart given in Table III.

Twelve processing runs are summarized in Table IV. The cathode patterns are shown in Fig. 23 .

The processing efforts can be divided into four main parts:

- a. Early runs with existing mask sets.
- b. Runs designed to test the effects of non-mask-related variables.
- c. Runs to evaluate the effects of the first new mask set.
- d. Runs to evaluate the second new mask set.

TABLE III  
Process Outline

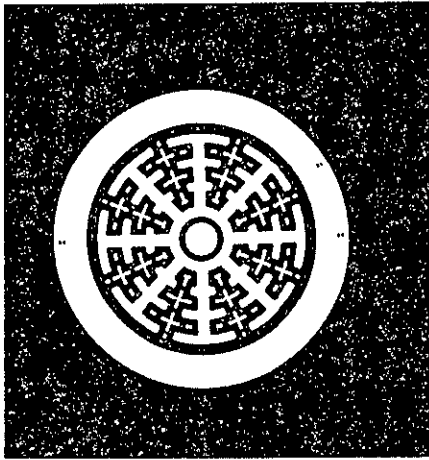
---

Silicon slice preparation  
p-type diffusions  
Oxidation  
Photomasking  
n-type diffusion  
Photomasking  
Contacting  
Edge bevel, etching, and passivation  
Packaging

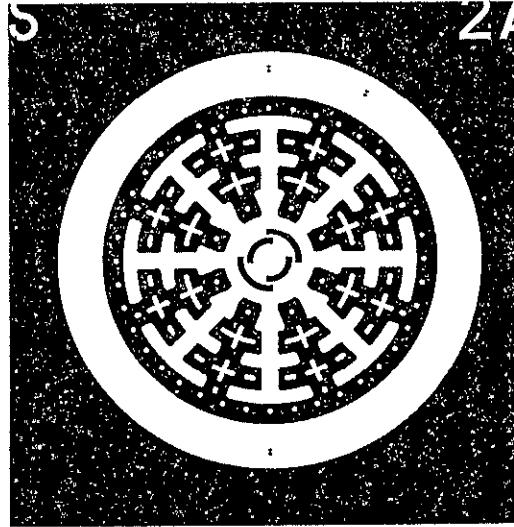
---

TABLE IV  
Summary of Process Runs

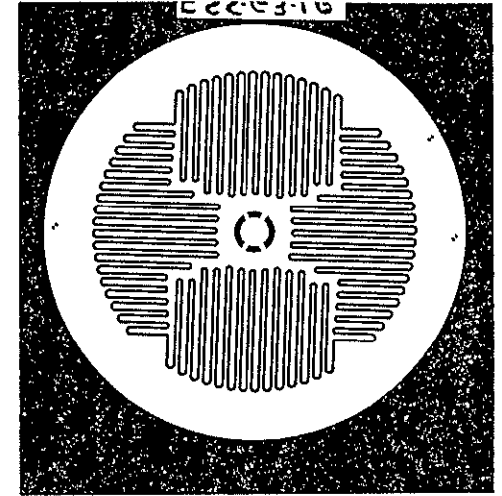
Run No.	Cathode Pattern and Slice Diameter	Where and How Processed	Features
1	1, 23 mm	Production	Showed that a device with a shunted cathode and gate amplification performed better than previous GATT devices without these features.
2	1, 23 mm	Production	Same as 1, with thinner slices for lower $V_{TM}$ and including samples with pattern/without shunts.
3	2, 33 mm	Production	Larger slice diameter to decrease $V_{TM}$ .
4	1, 23 mm	Research	Research process and a different lifetime killing technique.
5	1, 23 mm	Production	Lower slice resistivity.
6	3, 33 mm	Production	New mask design.
7	3, 33 mm	Research	New mask design.
8	3, 33 mm	Production	New mask design with extra bypass diode diffusion.
9	3, 33 mm	Production	Second new mask design.
10	3, 33 mm	Production	Same as Run No. 8.
11	3, 33 mm	Research	Same process as Run No. 8.
12	3, 33 mm	Production	Same as No. 8, various working points.



Mask No. 1  
23 mm dia.



Mask No. 2  
33 mm dia.



Mask No. 3  
33 mm dia.

Fig. 23 - Cathode patterns

## 7. EXPERIMENTAL RESULTS AND DISCUSSION OF RESULTS

The significant results of the measurements made on the devices are given in this section. This information is presented in the order in which it was generated with the Process Run Number in which the devices were made. The significance of the findings is discussed for each case.

### Run No. 1

Data were taken on devices of the GATT design used in the previous NASA sponsored program (Contract No. NAS3-14394) and a design that has yielded good fast, non-gate-assisted, thyristors (Mask No. 1). These data show:

1. That the devices made with Mask No. 1 yielded faster turn-off times and lower forward drops than the devices of the previous GATT design.
2. A gate-assist current of only 3  $\mu$ sec pulse width, as called for by the contract, is not effective for decreasing the turn-off time if the gate-assist pulse is not coincident with the reapplication of forward voltage.

### Run No. 2

Data from this run showed that thinner slices could be used to achieve a lower forward drop without sacrificing the required blocking voltages.

Two short, but quite valuable, empirical studies were performed in which the voltage of the floating digitated gate was observed during turn-off time measurements.

1. Thyristors were fired in a mode in which the gate firing current was fed into the digitated gate electrode that is normally floating with the main center gate open. After several hundred microseconds, the anode current was commutated to zero. About ten microseconds after  $I = 0$ , a forward anode voltage ramp was reapplied. This voltage ramp induced a voltage pulse between the center gate and floating gate of the order of 0.7V, i.e., a forward bias pulse was produced on the auxiliary cathode that was capable of firing the auxiliary thyristor and limiting the turn-off time. This result demonstrates that the anode emits holes over its entire anode area and the importance of minimizing the excess charge in the gate areas of a thyristor.
2. If one varies the  $dV/dt$  of the reapplied forward anode voltage, one finds that the magnitude of the IR drop measured in the p-base that causes the device to fire depends on the pulse width of the forward recovery current. This pulse width depends on the applied  $dV/dt$  as was shown in Fig. 1'

The significance of these findings is included in the discussion of the physical model for turn-off in Section 5.

Other data taken on devices from Run No. 2 showed that the objective of no more than 12 mJ per pulse dissipation for the device is feasible. Work in this area prompted study of the forward recovery behavior and losses. The results of this study were presented at the 1974 Meeting of the Industrial Applications Society of the IEEE. (7)

### Run No. 3

The purpose of this run was to achieve a lower forward drop by the use of a larger slice without degrading the turn-off time. The

results of this run were initially very disappointing because for a given lifetime level the devices had both a higher forward drop and a lower turn-off time. These surprising results were studied and lead to two very significant findings:

1. It was found that the p-type diffusion process had not yielded the desired profile. This prompted a review of a considerable body of data to see how variations in the p-type diffusion affect the  $V_{TM}-t_q$  tradeoff. This study revealed a correlation between the density of the acceptor atoms in the p-base under the n-type cathode and the  $V_{TM}-t_q$  tradeoff as shown in Fig. 24.

It was known at the start of the program that as one varies the carrier lifetime, the  $V_{TM}-t_q$  relationship varies as shown in Fig. 24. At relatively high lifetimes, a reduction in lifetime has much greater effect on  $t_q$  than on  $V_{TM}$ . At relatively low lifetimes, the situation is reversed.

A simple consideration of the device physics yields the understanding that decreasing the acceptor density in the p-base will decrease the  $V_{TM}$  and increase the  $t_q$ . Given this, it is reasonable that one should choose this acceptor density with a consideration of where one plans to be in the relationships illustrated by Fig. 24. If one is in the area where  $t_q$  changes rapidly and  $V_{TM}$  changes slowly—the region in which most commercial thyristors are in— $t_q$  is the greater problem and one should choose a relatively high acceptor density to decrease the  $t_q$ . On the other hand, for a fast thyristor of the type being developed on this program, the



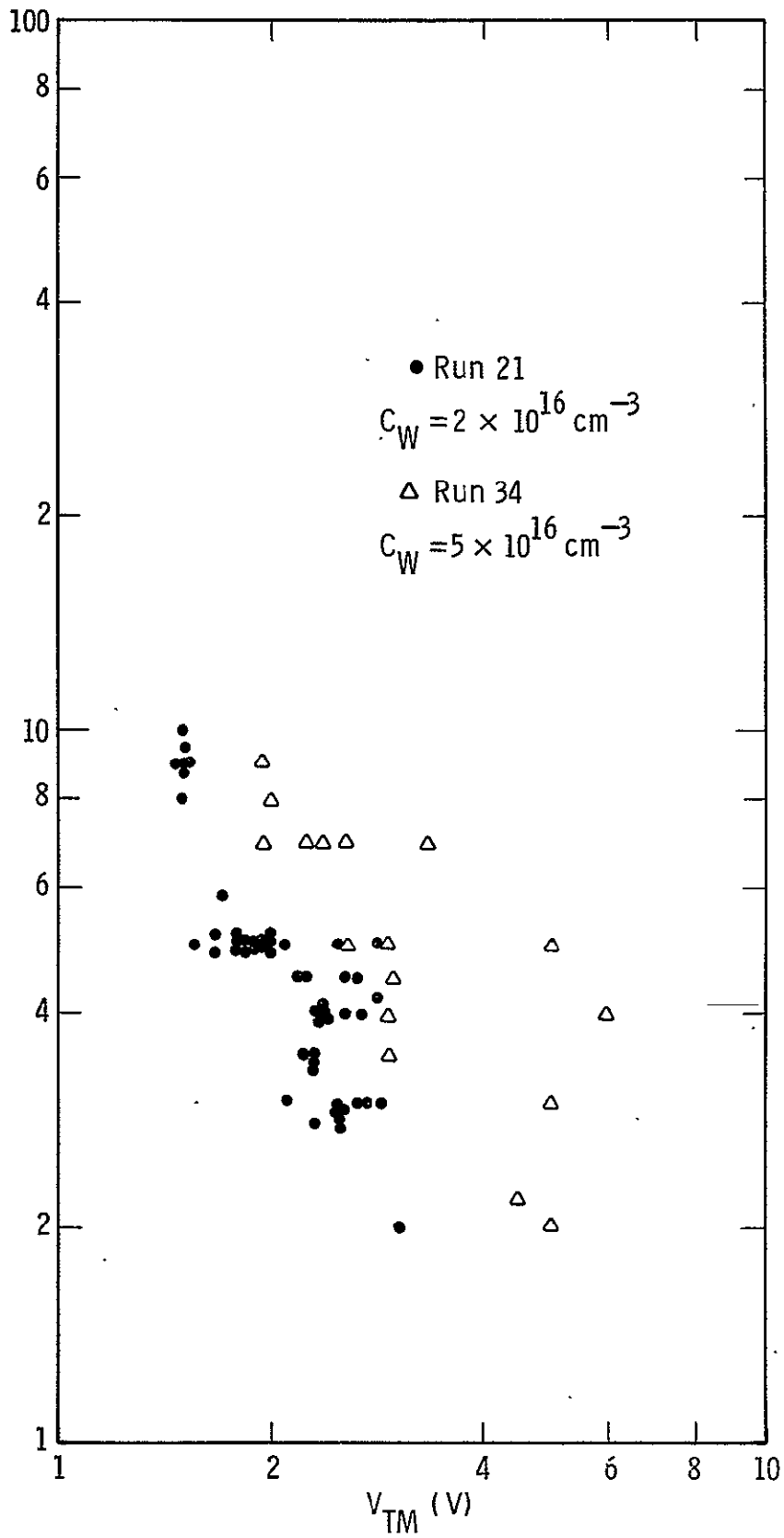


Fig. 24 —Effect of P-layer working point ( $C_W$ ) on  $t_q - V_{TM}$  trade-off

$V_{TM}$  is more strongly affected by changes in lifetime than is  $t_q$ . This calls for a lower acceptor density.

The fact that one should not use the same acceptor density for devices over the entire range of turn-off speeds was not evident from the existing theory.

2. The observation that these devices had a higher  $t_q$  than expected lead to a significant increase in understanding the effect of cathode geometry on  $t_q$ . These devices were made with cathode patterns that were essentially an enlarged version of those of the earlier runs. This lead to the realization that the gate area must be kept small to minimize the amount of excess charge that must flow from the gate regions during turn-off. Also this lead to the understanding that a wider cathode line causes a higher resistance in the p-base under the cathode, and this increases the  $t_q$ . Thus the devices from Run No. 3 played a big part in improving our understanding of device behavior as given in Section 5.

#### Run No. 4

The purpose of this run was to determine whether a better  $V_{TM}$ - $t_q$  tradeoff could be obtained by using a different lifetime killing technique. It is conceivable that differences in capture cross section and position in the energy gap due to differences in the lifetime killing technique can affect  $V_{TM}$  and  $t_q$  differently. The results of this run were inconclusive.

Run No. 5

The blocking voltages of the thyristors from this run were too low ( $\sim 600V$ ) due to the lower slice resistivity.

Runs No. 6 and 7

These two runs, each having mask design No. 2, were made in parallel, one at the Research Center and one at the Semiconductor Division, to minimize the time it would take to get the first results with the new mask design.

Devices from these runs showed that the integrated bypass diode would provide the low resistance path to bypass the amplifying gate structure. On the other hand, these devices showed the problem that the integrated diode would fire the thyristor when gate-assist current was drawn. This problem had been expected but not to the degree that it was found. The results from this run lead to the modification in design described on pages 18, 22, and 23.

Run No. 8

The devices from this run provided the first successful demonstration of the feasibility of the integrated bypass diode.

Run No. 9

This run was aborted because the desired diffusion profiles were not achieved.

Run No. 10

This run has provided the first devices with new mask design No. 3. A photograph of one of these devices is shown in Figure 25.

Data taken on these devices has shown the following:

1. As expected, these thyristors have a significantly faster turn-off time. For example, at a given

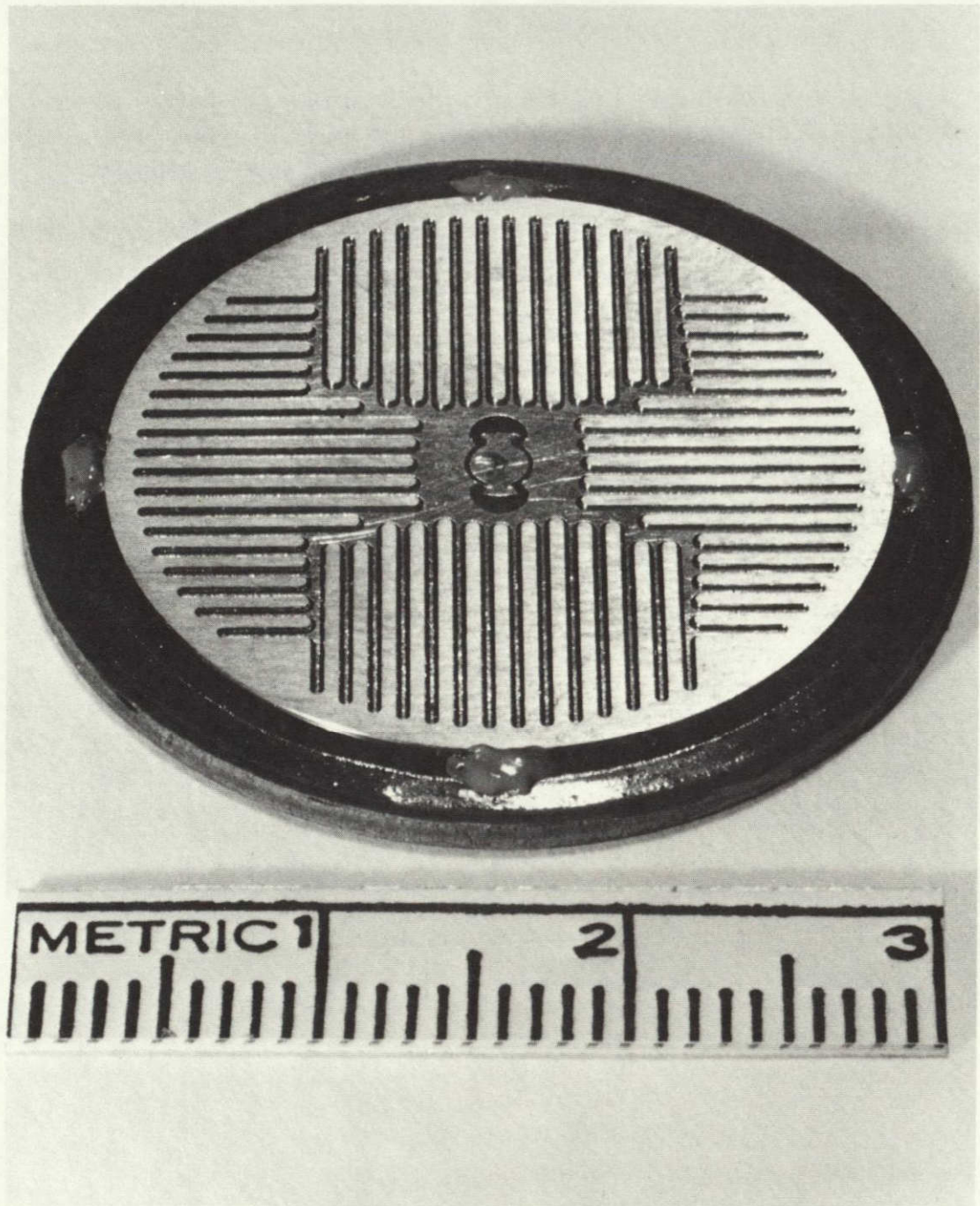


Fig. 25 - Photograph of a device made with Mask No. 3

lifetime control level the new devices turn-off (conditions specified in Table I except that there is no gate-assist current) in 6 to 8 microseconds in contrast with 18 to 24 microseconds for the best previous devices. At a lower lifetime level, the new devices turn-off in 2.5 to 3.0  $\mu$ sec in contrast with 7 to 10  $\mu$ sec on the earlier devices.

2. An unexpected result was that 2 amps of gate-assist current does not effectively decrease the  $t_q$ . This surprising result lead to the understanding that if gate-assist current is to be effective, it must create a voltage in the p-base that is roughly equal to or larger than 0.7 volts. This is described in detail under the Physical Model for thyristor turn-off on page 49. The proposed solution to this problem is to change the diffusion profile to increase the resistance under the cathode.
3. The minimum gate current and voltage to fire and the latching and holding currents are quite similar to those of devices of old design. Typical values are:

	<u>Measured</u>	<u>Required</u>
$I_{GT}$	70 to 160 mA	< 200 mA
$V_{GT}$	0.9 to 1.0V	< 4V
$I_{LX}$	300 to 400 mA	--
$I_H$	100 to 120 mA	< 200 mA

4. Thirty-one out of thirty-five of these devices have forward blocking voltages between 800 and 1300V. Twenty-seven were between 1000 and 1300V. Unfortunately, only about 20% of these devices have reverse blocking voltages between 800 and

1200V. The low reverse blocking voltages are due to improper anode alloying procedures and are not related to the new device design.

5. The bypass diode of these devices refires the devices in the gate-assist mode. This has been observed in earlier devices and is solvable with a locally decreased lifetime.
6. The measured forward drops were between 1.8 and 2.7 volts (at the lifetime level that yielded 6 to 8 microsecond turn-off times). The contract calls for a maximum of 2.5 volts. The 23 mm snowflake devices had a forward drop of 1.5 volts at the same lifetime level. The unexpected higher forward drops can, in hindsight, be explained as follows. The long narrow cathode geometry reduces the npn alpha, and this lower alpha causes a higher forward drop in the same way as a lower lifetime causes a higher forward drop. It is expected that when the planned change in the working point is made, this will bring the alpha back up and the forward drop back down.
7. The forward drop seems to be much less dependent on the anode current than previous devices were all the way up to 800 amps. The significance of this remains to be determined. It could mean that this is a better high current device; or on the other hand, it may mean that one should have a smaller device for the specified 200 amps. With the very narrow cathode lines, perhaps the effective shunt area significantly reduces the cathode area. If so, it is not clear if this is

good or bad. Recent information both from Siemens and from our own Labs indicates that, at least during the turn-on transient, making the current density higher has some good effects. In any event, the understanding of thyristor behavior should be advanced by the study of this unexpected finding.

Run No. 11

These slices are at the metallization step; and, therefore, there are no test results.

Run No. 12

These slices are being run in small lots for different phosphorus diffusion times. Two such lots have been carried to near completion. One is at the edge preparation step, and the other is at the metallization step.

## 8. REVIEW MEETING AND DEVICE DELIVERIES

A meeting was held May 2, 1974, at NASA-Lewis Research Center to review the findings to date. In addition to the people directly involved with the program from NASA and Westinghouse, the meeting was attended by other interested NASA personnel, TRW personnel involved in developing the circuits in which the thyristors are to be used, and JPL personnel involved in one of the missions in which the circuits are to be used. The possibilities of improving the overall performance and characteristics of the circuit were reviewed in detail. Eight thyristors (which nearly met the objectives of contract as shown by the data of Table V), along with their electrical characteristics, were supplied to NASA at this meeting. Westinghouse proposed two possible courses of action to NASA:

1. Fabricate and deliver additional thyristors similar to the eight represented by Table V. This could be done rather quickly within the program.
2. Continue development work utilizing information obtained on the program and at the meeting to develop the best device attainable. This would require a six-month extension of the contract but within the contract cost.

NASA chose the second option. A separate contract (NAS 3-19097) was negotiated for an additional 35 thyristors similar to the eight supplied at the meeting except with a slightly different forward-drop turn-off time tradeoff. These devices were delivered and their performance data are given in Table VI.



TABLE V

Characteristics of the Eight Devices Loaned to NASA

Devices	$t_{off}$			$V_{TM}$	$V_{DRM}$	$V_{RRM}$	$I_{GT}$	$V_{GT}$	$I_H$	$I_{LX}$	dV/dt	Energy Pulse	Units
	$\mu\text{sec}$	$\mu\text{sec}$	$\mu\text{sec}$	V	V	V	mA	V	mA	A	V/ $\mu\text{sec}$	mJ	
21-2	5.5	3.0	5.5	2.9	1180	1040	130	1.25	65	0.5	> 500	12	
21-19	6.0	3.5	6.0	2.3	1080	940	100	1.10	55	0.4	> 500		
21-26	6.5	3.0	6.5	2.1	1100	1080	90	1.10	50	0.4	> 500	11	
21-49	6.5	5.0	6.5	2.1	920	920	120	1.10	55	0.5	> 500		
21-55	5.5	4.5	5.5	2.2	740	680	100	1.00	55	0.4	> 500		
21-4	8.0	4.0	8.0	2.4	720	680	85	1.10	40	0.4	> 500		
21-42	5.0	5.0	5.0	2.5	890	840	100	1.10	70	0.8	> 500		
21-30	5.0	4.5	5.0	2.2	830	760	130	0.95	65	0.4	> 500		
Conditions													
temp	100	100	100	100	100	100	25	25	25	25	100		$^{\circ}\text{C}$
$I_{TM}$	200	200	200	200									A
-diR/dt	25	25	25										A/ $\mu\text{sec}$
dV/dt	400	400	400										V/ $\mu\text{sec}$
VRev	yes	yes	yes										V
Gate I	2	2	0							2			A
Gate PW	3	10								3			$\mu\text{sec}$
$I_A$					0.01	0.01							A
$V_A$							30	30	30	30			V

TABLE VI  
 Characteristics of Thyristors Delivered on NASA Contract No. NAS3-19097

Conditions	$t_{off}$			$V_{TM}$		$V_{DRM}$	$V_{RRM}$	$I_{GT}$	$V_{GT}$	$I_{LX}$	$I_H$
	$\mu\text{sec}$	$\mu\text{sec}$	$\mu\text{sec}$	V	V	V	V	mA	V	mA	mA
Temp., °C	100	100	100	100	100	25-100	25-100	25	25	25	25
$I_{TM}$ , A	80	200	200	80	200						
$-dI_R/dt$ , A/ $\mu\text{sec}$	10	50	25								
$dV/dt$ , V/ $\mu\text{sec}$	50	400	400								
Gate: I, A	2	2	2								
PW, $\mu\text{sec}$	10	10	10					10	10	10	
Device Nos.											
54	4.2	7.9		1.50	1.85	1000	960	120	1.4	870	168
55	4.1	8.0		1.98	1.96	1100	1080	150	1.5	1350	200
56	4.0	9		1.96	2.07	1280	1120	120	1.2	900	150
57	5.0	8.4		1.75	2.05	1120	1030	300	2.0	1900	190
63	5.0	9		2.00	1.98	1260	1120	180	1.6	1500	320
64	4.0	7		1.74	2.01	960	960	120	1.2	700	180
65	4.0	7.2		1.80	1.97	1000	1000	125	1.4	1050	170
66	4.0	8.4		1.41	1.75	940	930	160	1.5	1200	300
70	6.4	11	11	1.86	2.05	990	960	150	1.3	790	260
71	3.5	5.8	5.0	1.57	1.89	1200	1120	160	1.5	1300	280
74	4.1	8.2		1.72	2.16	1100	1000	170	1.7	2200	340
77	4.0	16	9	1.43	1.77	900	920	120	1.2	1300	320
78	3.8	13	7	1.49	1.90	1200	1000	120	1.2	750	200
82	< 3.0	5.8		1.79	2.14	1010	1020	200	1.6	1500	320
86	4.0	9		1.40	1.75	1200	1040	120	1.2	1000	190

TABLE VI (Continued)

Device Nos.	$T_{off}$			$V_{TM}$		$V_{DRM}$	$V_{RRM}$	$I_{GT}$	$V_{GT}$	$I_{LX}$	$I_H$
108	4.1	1.5		1.45	1.84	900	800	150	1.3	1150	220
110	4.0	12		1.35	1.63	1080	1090	120	1.2	850	180
120	4.2	12	8.2	1.43	1.70	1260	1120	130	1.6	1000	170
124	3.2	8		1.49	1.95	880	890	130	1.2	1150	320
128	3.2	7.2		1.45	1.67	1000	960	160	1.2	1500	230
132	3.0	7.6		1.69	2.13	1000	1000	160	1.4	1600	280
135	4.4	9.8		1.70	1.89	1080	1080	150	1.6	1600	250
137	4.0	6.4		1.45	1.80	1120	920	130	1.4	1300	210
138	4.2	10	9	1.43	1.75	1020	1040	120	1.4	1160	210
139	4.0	7		1.54	1.96	1220	880	160	1.6	1200	210
140	4.5	7.5		1.52	1.77	980	990	140	1.2	900	200
141	5.0	8		1.88	2.18	1200	1200	210	1.6	2000	400
122	12.	V. high		1.17	1.47	920	960	100	1.0	380	160
143	4.2	7.2		1.60	2.11	1160	1080	180	1.6	2200	210
144	3.6	7.8		1.68	1.96	880	880	140	1.6	1350	250
145	4.2	10.2	9.8	1.47	1.77	960	960	150	1.7	1250	240
131	12.	32	19	1.22	1.44	830	840	80	1.0	450	120
148	4.5	14	8	1.34	1.62	760	720	150	1.2	1200	210
149	5.0	17	13	1.65	1.89	960	880	150	1.4	1200	230
152	4.0	6.4	6	1.51	1.86	1120	1080	120	1.3	720	150
153	4.2	9		1.37	1.69	1020	1020	100	1.2	700	150
154	7.0	11.2	10.4	1.50	1.79	1000	920	120	1.4	1180	160

## 9. SUMMARY OF RESULTS

An improved gate-assisted turn-off device has been developed. Performance improvements include:

1. A decrease in the turn-on gate current from more than 15A to only 2A.
2. A decrease in the gate-assist current from more than 10A to only 2A.
3. A decrease in the energy loss per pulse from 30 mJ to 12 mJ.
4. The current rating was increased from 100 to 200A.
5. The need to have a gate-assist current on continuously to prevent firing by an unexpected  $dV/dt$  was eliminated, i.e., the  $dV/dt$  rating \_\_\_\_\_ without gate-assist current was improved by two orders of magnitude.

The reliability of the thyristor was improved by:

1. Eliminating an important failure mode of gate-assisted turn-off thyristors.
2. Decreasing the heat dissipation of the device.
3. Integrating a bypass diode into the silicon slice.

These improvements were achieved by means of the following device design features:

1. Gate amplification and cathode shunting were incorporated into a gate-assisted thyristor.

2. A new technique was devised that makes it practical, in a three-terminal thyristor, to combine gate amplification and gate-assisted turn-off in the same device.
3. The gate-cathode geometry was improved.
4. The diffusion profile was improved.

These design changes were made possible by the development of a better understanding of how thyristors turn-off both with and without gate-assist. The problems involved with making accurate measurements of turn-on speed and losses have been better defined.

Two research areas have been identified that promise to yield a significant improvement in device performance. They are:

1. It was demonstrated that the  $V_{TM}-t_q$  tradeoff can be improved by changing the working point in the p-base diffusion profile. This interdependence should be better defined to establish a basis for choosing the best working point for a given  $V_{TM}-t_q$  tradeoff.
2. More accurate measurements should be made of the turn-on switching losses. The effects on these losses of test conditions and of variation in the cathode boundary length should be determined to provide a basis for choosing the length in a new thyristor design.

NASA has provided a contract extension to pursue the above research areas. The modification also includes a design study of thyristor packaging approaches to reduce device/heat sink weight and to improve heat transfer from the thyristors to the heat sink. Prototype quantities of thyristors and packages will be delivered incorporating the improvements resulting from these studies.

## REFERENCES

1. F. C. Schwarz, "A Series Capacitor Inverter-Converter for Multi-kilowatt Power Conversion," NASA Technical Report, NASA TR R-336, 1970.
2. T. P. Nowalk, J. B. Brewster, and Y. C. Kao, "High Voltage and Current, Gate-Assisted, Turn-Off Thyristor Development," Final Report NASA Contract No. NAS3-14394.
3. D. R. Hamilton, J. B. Brewster, W. D. Frobenius, and T. Desmond, "Development of a High Speed Power Thyristor—The Gate-Assisted Turn-Off Thyristor," Final Report, NASA Contract No. NAS12-2198.
4. P. Voss, "The Turn-On of Thyristors with Internal Gate Amplification," IEEE Conference Record of the 1974 Ninth Annual Meeting of the Industrial Applications Society, pp. 467-476.
5. F. E. Gentry, et al., Semiconductor Controlled Rectifiers, Prentice Hall, page 34.
6. H. B. Assalit and G. H. Studtmann, "Description of a Technique for the Reduction of Thyristor Turn-Off Time," IEEE Trans. Electron Devices, Vol. ED-21, pp. 416-420, 1974.
7. J. B. Brewster and E. S. Schlegel, "Forward Recovery in Fast Switching Thyristors," IEEE Conference Record of the 1974 Ninth Annual Meeting of the Industry Applications Society, pp. 663-672.